Miniaturization of a Low Power Harmonic Radar for UAV use

SALEH A.ALJASER
MASTER´S THESIS
DEPARTMENT OF ELECTRICAL AND INFORMATION TECHNOLOGY
FACULTY OF ENGINEERING | LTH | LUND UNIVERSITY

Master Thesis
Miniaturization of a Low Power Harmonic Radar for UAV use

Saleh A.AlJaser
saleh.aljaser.0737@student.lu.se

Department of Electrical and Information Technology
Lund University

Supervisor: Anders J Johansson

Examiner: Fredrik Rusek

June 14, 2019

Abstract

The aim with this Master thesis work is to design, build and test a small size, light weight and low power consumption harmonic radar system that will be installed in a flying drone for the purpose of tracking and localizing tagged Bogong moths near their aestivation caves and crevices in Australia during summer. A FMCW harmonic radar is proposed, it comprises a radar transmitter, receiver and a signal processor. The challenges of the design are to make the system small and light enough to be carried by the drone and to keep power consumption as low as possible to at least complete an entire search mission with one battery charge. The investigations during the thesis cover link budget analyses for different design options, operating frequency selection, waveform design, system simulations and components selection. The moths are tagged with a special adhesive tag which is small so it does not disrupt the insect movement, the small size and low reflected power of the tag limits the radar detection range and the radar design is optimized to improve range measurement by proper selection of components and proper design of the radar waveform.

Acknowledgements

Popular Science Summary

In Australia nearly two billion Bogong moth migrate twice every year for hundreds of kilometers. They migrate in spring from different parts of Australia to the Australian Alps looking for cold weather, they stay in the mountains for four months during summer. They get back in the beginning of autumn to their original places. When they reach the cold mountains in the south they start their aestivation period gathering in large numbers on the walls of the caves on the mountains sides and under tree trunks, there are about 17000 moths per square meter on these walls. Finding Bogong moths is very important for researchers to study the way that they navigate during their night time migration. However, finding them is challenging and can be only by luck since it requires climbing the mountains sides and searching thoroughly in all crevices and small openings in the rocks [5].

Researcher makes use of special pieces of equipment to search and locate the moths under the rock, tree trunks and inside the caves. One way to do so is by using radars. A radar is a radio transceiver system that transmits a special electromagnetic signal and then listens to the reflections of that signal from the surrounding environment. It measures the time difference between the transmitted and reflected signals to calculate the objects ranges. Radars have been used before to detect different flying and ground insects and found to be effective, however there are several challenges of detecting small insects since radars relay on the reflected signal power from targets of interest, and the smaller the target is the weaker the reflected power to the radar, one other problem is the reflections from other unwanted objects around the target which can mask the target reflections, they are called clutter.

In this thesis we attempt to investigate the use of radars to detect Bogong moths. The idea is to use special type of radars called Harmonic Radars that use the fundamental signal frequency for transmission and the second signal harmonic for reception to get some sort of clutter immunity and highlight the Bogong moth by tagging it with a special adhesive tag. The system is then designed, built and tested as a proof of concept for the Bogong moth detection.

Contents

List of Figures

List of Tables

Glossary

ADC Analog to Digital Converter. 8, 21–23, 38, 41, 47, 54–56, 66, 70, 71

AGC Automatic Gain Control. 7, 55, 56

BPF Band Pass Filter. 7, 22, 52, 54, 69

C-BAND Frequency band from 4 GHz to 8 GHz. 14

CW Continuous Wave. 6, 29, 35, 37, 38

D_R Duty Ratio. 29

DAC Digital to Analog Converter. 21–23, 38, 47, 51, 55, 56, 66, 69, 71

dB Decibel. 11, 12, 41

DC Direct Current. ix, 6, 40, 46, 51, 53, 54, 57, 58, 60

EIRP Effective Isotropic Radiated Power. 19, 24, 25, 33, 44

EM Electromagnetic. 8, 9, 11, 59

FMCW Frequency Modulated Continuous Wave. i, 38–41, 45, 49, 71

HMI Human Machinery Interface. 8

IF Intermediate Frequency. 7, 8, 22, 27, 54

IM Inter-Modulation. 7, 21, 22

IQ In-phase Quadrature-phase. 21, 23, 54

IQ-DEMOD In-phase Quadrature-phase De-modulator. 21, 23

ISM Industrial, Scientific and Medical. ix, 18–20, 22, 24, 41, 43, 44, 46, 52

K-BAND Frequency band from 18 GHz to 27 GHz. 14

LNA Low Noise Amplifier. x, 7, 53, 54, 67–69

LO Local Oscillator. 6, 21, 23, 52, 54, 58, 59, 70

LoS Line of Sight. 25

LPF Low Pass Filter. 7, 24, 54

MCU Micro-controller Unit. 24

OP-AMP Operational Amplifier. 47, 57

PA Power Amplifier. 6

PLL Phase-Locked Loop. ix, 24, 47–53, 56, 57, 59, 71

PPI Plan Position Indicator. 8

PRF Pulse Repetition Frequency. 29, 31

PRI Pulse Repetition Interval. 29–31, 34, 35, 45

RCS Radar Cross Section area of the target. 10, 12

RF Radio Frequency. vii, 6, 7, 14, 15, 20, 21, 29, 38, 46–50, 52, 54, 57, 58, 60, 67, 71

RX Receiver. x, 12, 14, 15, 18, 21, 23, 25, 29, 44, 52, 54, 55, 58, 67–69, 71

SNR Signal to Noise Ratio. ix, 8, 10, 24, 25, 27, 31–33, 38, 41, 45, 71

SSB Single Side Band. 46

STC Sensitivity Time Control. 7

TCXO Temperature Compensated Crystal Oscillator. 24, 48, 49

TX Transmitter. x, 12, 14, 15, 18, 20–22, 24, 25, 27, 29, 44, 45, 52, 54, 56, 58, 59, 66, 67, 69, 70

UAV Unmanned Air Vehicle. 1, 18, 71

VCO Voltage Controlled Oscillator. ix, 21–24, 46–52, 56–60, 71

X-BAND Frequency band from 8 GHz to 12 GHz. 14, 57

Introduction

Harmonic radars are useful for detecting small objects from long distances, since they can distinguish the reflected signals of the special tags from the clutter of the surrounding environment. They work by transmitting a radar signal at a certain frequency of operation then the tag placed on the target of interest reflects the signal at the second harmonic of the transmitted frequency, this is achieved by designing a special tag comprising a resonant antenna and a non-linear element to generate the harmonic frequency. The reflected signal to the radar receiver is at twice the frequency of the transmitted signal, while the clutter which is the reflections from the surrounding environment is reflected at the same frequency as the transmitted signal that makes it easy for the radar receiver to filter the signal of interest from the unwanted interference.

In this project the aim is to investigate, design, manufacture and test a harmonic radar with given specifications to be used to detect a tagged Bogong moth from at least 30m ranges. The investigations include frequencies of operation and legislation, design approaches, radar wave-forms, system requirements and components selection.

The outline of this thesis is as follow:

Chapter 2 gives a literature study of insect tracking and the use of Harmonic radars, it also covers the basic concept of radars in general and the required theory.
Chapter 3 explains the high level analysis and requirements study, it covers different system concepts and performs comparisons.
Chapter 4 introduces different radar wave-form designs.
Chapter 5 covers in details the design of all system components with simulation results and required theory.
Chapter 6 shows the system's manufacturing, assembly and integration processes.
Chapter 7 shows the testing and verification of the radar system.
Appendices include MATLAB codes and CAD drawings.

Background and Literature Study

2.1 Radar Basics

Radars are sensors that use radio waves to detect targets' ranges and velocities. Targets can be anything that reflects radio waves, such as air crafts, ships, vehicles, clouds, birds, or even insects [14].

A basic radar system consists of a transmitter, a receiver and a radar signal processor. A basic radar block diagram is shown in Figure 2.1. The diagram shows
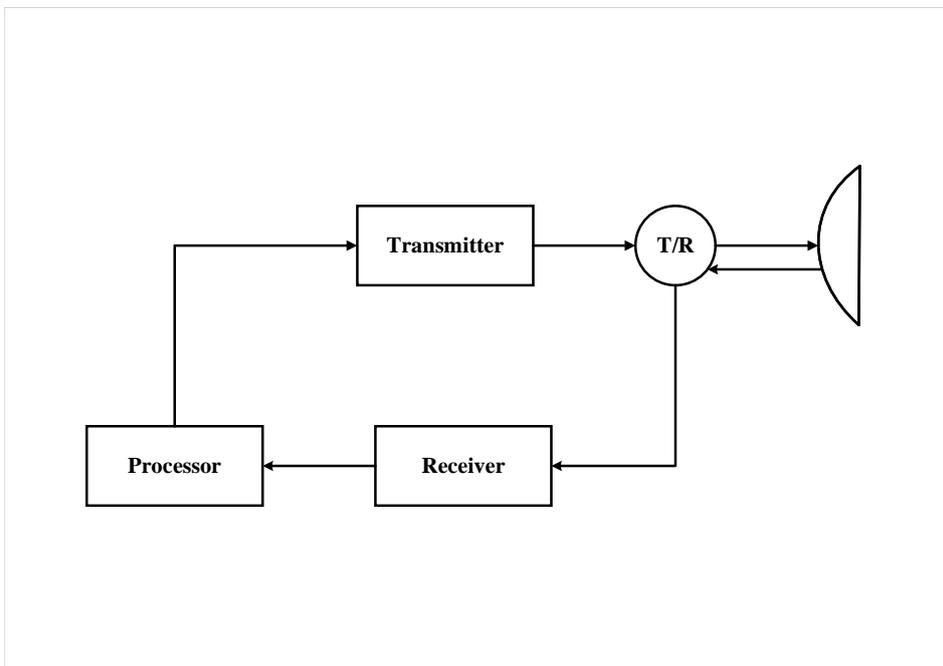
Figure 2.1: Basic Radar Block Diagram.

the major blocks of a radar system.

2.1.1 Transmitter

A radar transmitter is responsible for generating the RF signal required for the target detection. The transmitter usually comprises an oscillator which generates the reference source for the RF signal, a modulator which works at low frequencies to modulate the source signal with a modulation signal, an up-converter which converts the modulated signal to the required RF transmit frequency and a power amplifier PA which amplifies the transmitted signal to the required transmit power. A basic transmitter block diagram is shown in Figure 2.2. Radar transmitters can
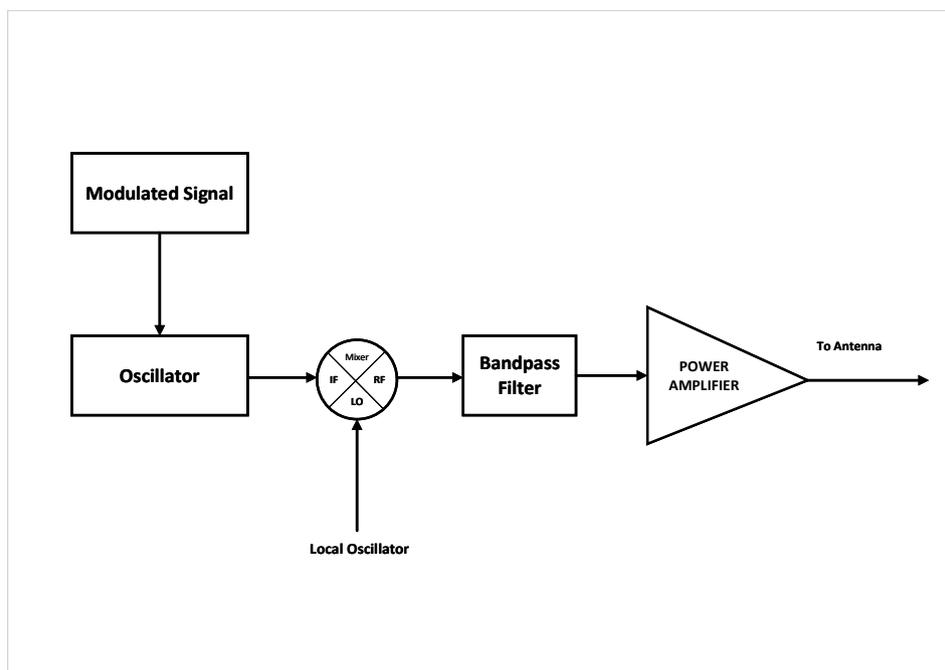
Figure 2.2: Radar Transmitter Block Diagram.

be made pulsed or continuous wave CW depending on the application. Pulsed radar transmitters usually have ultra high peak RF powers and are active only in a short period of time where pulsing can be made by switching the DC supply of the transmit PA ON and OFF [14]. Other modulation techniques can still be used within the transmission period by modulating the oscillator amplitude, phase or frequency.

CW radar transmitters are active all the time allowing for higher average transmit powers compared to pulsed transmitters, however peak powers are usually limited due to receiver leakage and overheating limitations [14]. Similar modulation techniques can be implemented on CW transmitters by modulating the oscillator. Further information about pulsed and CW radars will be discussed later in Chapter 4. The oscillator is usually known as the radar exciter which is a very stable oscillator with low phase noise. The exciter is used as well for the receiver local oscillator LO to perform down-conversion. It is also used as a clock for the

receiver/transmitter synchronizations. This is the reason of usually combining it with the radar receiver subsystem.

2.1.2 Receiver

A radar receiver is responsible for receiving the reflected waves from targets, amplifying the low signal levels with minimum additional noise, translating them to base-band frequency (provides down-conversion), and sometimes converting the analog base-band signals into digital domain if required by the signal processor. A basic radar receiver block diagram is shown in Figure 2.3. The receiver com-
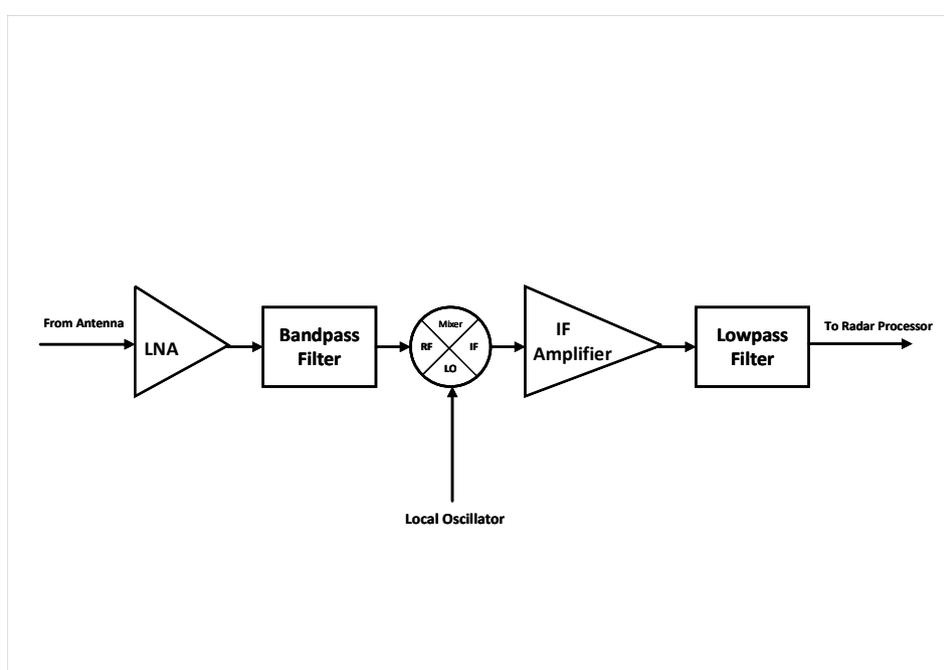
Figure 2.3: Radar Receiver Block Diagram.

prises a low noise amplifier LNA, a RF band-pass filter BPF, a down-converter, an intermediate frequency IF amplifier and a base-band low-pass filter LPF. The LNA amplifies the received RF signal while adding minimum noise to the signal, this can be achieved by matching the amplifier chip to the minimum noise figure operating point. The RF BPF is used to suppress the out of band noise and interference to improve the receiver signal to noise ratio (SNR). The mixer is used as a down-converter to translate the RF signal into IF frequency or directly to base-band depending on the receiver topology. The IF amplifier is used to further amplify the received signal to the required level for driving the digital to analog converter, this amplifier usually has more functionality than just amplification such as variable gain as in Automatic Gain Control AGC or Sensitivity Time Control STC applications. The LPF is used to filter the base band signal from the inter-modulation IM mixer outputs. Moreover, the base-band bandwidth of the IF

filter is used to set the receiver bandwidth and calculate the receiver noise power [12].

2.1.3 Processor

The radar processor is responsible for making decisions on the received signals by assigning reflections to targets or noise, interference and clutter. All radar algorithms and identification lookup tables are stored and performed in the radar processor starting from SNR calculations to range, velocity measurements and processing gain algorithms including correlators and de-modulators. Depending on the system configuration the user interface HMI can be included in the radar processor connecting the received IF or digital signals to target visualisations in a user friendly plan position indicator PPI. Most of the processor components are digital, however in some configurations it can include an analog to digital converter ADC which accepts analog signals from the radar receiver and performs sampling, quantization and digitization.

2.1.4 Radar Parameters

As mentioned in previous sections radars work by transmitting a known electromagnetic EM wave and receive the reflection from surrounding objects. It is known that EM waves travel in air at the speed of light, then the target range can be calculated from the time required for the EM wave to be reflected back to the radar receiver using the following equation [14]:

$$R = \frac{c\Delta T}{2} \tag{2.1}$$

Where

- c is the speed of light and equals to 3×10^8 m/s.

- ΔT is the two way propagation time to the target and the division by 2 is to find the one way distance to the target.

Target velocity can be calculated from the Doppler shift on the reflected EM wave. Doppler shift is a result of relative motion between the radar and the target. Reflected EM wave from the target will have slightly different frequency compared to the transmitted wave; this can be clearly observed in acoustic waves, when a moving ambulance is approaching an observer the siren sound will have a higher pitch which means higher frequency, but when the ambulance is moving away from the observer the sound will have a lower pitch which means lower frequency as compared to a non moving ambulance. The target velocity can be calculated from the Doppler shift using the following equation [14]:

$$f_d = \frac{2f}{c} v_{target} \Rightarrow v_{target} = \frac{c}{2f} f_d = \frac{\lambda f_d}{2} \tag{2.2}$$

Where

- v_{target} is the radial component of the target velocity along the range dimension in m/s.

- f_d is the one way Doppler shift in Hz.

- c is the speed of light in m/s.

- $\lambda = \frac{c}{f}$ is the EM wave wavelength in m.

- f is the EM wave frequency in Hz.

- Division by 2 because the Doppler shift occurs twice; on the forward EM wave and on the reflected EM wave.

The radar ability to perform detection is dependent on the reflected powers from targets, they must be large enough to be identified by the radar receiver. The radar receive power can be derived easily from Friis transmission formula which is used in wireless communication systems to calculate the received power from the transmitted power density Q_i and the receiving antenna effective area. Power density of an isotropic radiator is defined equally on the surface area of a sphere around the radiator inversely proportional to the distance from the radiator. If the radiator is directive then the power density is stronger in the direction of higher directivity as shown in the following equation [14]:

$$Q_i = \frac{P_t G_t}{4\pi R^2} \tag{2.3}$$

Where

- P_t is the peak transmitted power in watts.

- G_t is the transmit antenna gain.

- R is the distance from transmitter in m.

- $4\pi R^2$ is the sphere surface area around the radiator.

The antenna gain is defined from the antenna effective area A_e as follows [14]:

$$G = \frac{4\pi A_e}{\lambda^2} \tag{2.4}$$

The antenna effective area is calculated from the antenna physical area and aperture efficiency η as following [14]:

$$A_e = \eta \cdot A_{phys} \tag{2.5}$$

Where η for typical antennas vary from 0.35 to 0.7. Then radar received power can be written as [14]:

$$P_r = \frac{P_t A_r A_t}{R^2 \lambda^2} = \frac{P_t G_t G_r \lambda^2}{(4\pi R)^2} \tag{2.6}$$

Where

- P_r is the received power by the radar system in watts.

- A_t and A_r are the transmit and receive antenna effective areas respectively.

The previous equation defines the received power at a distance R from the transmitter. This power will be reflected by the target with a reflection gain called Radar Cross Section RCS σ and then travel the same distance to the radar receiver, which is located at the same position as the radar transmitter; assuming Mono-static radar [14]. After adding all previous parameters, the radar received power can be expressed as [14]:

$$P_r = \frac{P_t G_t G_r \lambda^2 \sigma}{(4\pi)^3 R^4} \tag{2.7}$$

The radar receiver generates white random noise due to receiver temperature and other effects in the environment. This noise is white as mentioned so it covers all frequency bands with equal power; (uniformly distributed), it is random in amplitude and phase as well. Receiver noise limits the capability of target detection, the target reflected signal must exceed the noise power by a significant margin set by the required receiver Signal to Noise Ratio SNR. The receiver noise uniform power density P_n due to receiver temperature T_s can be calculated as follows [14]:

$$P_n = kT_0 FB = kT_s B \tag{2.8}$$

Where

- $k = 1.38 \times 10^{-23}$ is Boltzmann's constant.
- $T_0 = 290$ K is the receiver reference temperature in kelvin.
- F is the receiver noise factor ($T_s = T_0 F$).
- B is the receiver instantaneous bandwidth in Hz.

The SNR of the receiver is the margin of signal power over noise power. It has to be larger than 1 with a system requirement margin in order to be visible to the radar signal processor. SNR can be calculated by dividing the radar received signal power over the receiver noise power as follows [14]:

$$SNR = \frac{P_t G_t G_r \lambda^2 \sigma}{(4\pi)^3 R^4 kT_0 FB} \tag{2.9}$$

It is important to know that all receiver amplification stages amplify both received signals and generated noise, also receiver loss and attenuation lowers signal and noise levels according to the noise figure concept. The noise power is increased further by the total receiver noise figure. The total noise factor F can be calculated using the following equation [12]:

$$F = F_1 + \frac{F_2 - 1}{G_1} + \frac{F_3 - 1}{G_1 G_2} + \cdots + \frac{F_N - 1}{G_1 G_2 \cdots G_{N-1}} \tag{2.10}$$

Where

- $F_1, F_2, \cdots, F_N$ are noise factors of components in the receiver chain starting from the receiver front end.
- $G_1, G_2, \cdots, G_{N-1}$ are gains or ($\frac{1}{losses}$) of components in the receiver chain starting from the receiver front end.

Then the total noise figure can be calculated from the total noise factor by converting from ratio to dB. SNR analysis will be discussed in details with link budget analysis in chapter 5.

In addition to noise the radar receiver receives some unwanted interference due to other systems transmitting or leaking at the same frequency of operation either intentionally which is known as Jamming or unintentionally. Other interference can be due to reflections from the surrounding environment which is known as clutter. The clutter can be due to stationary or slowly moving targets such as tree leafs or clouds, then the Signal to Interference and Noise Ratio (SINR) can be calculated as [14]:

$$SINR = \frac{P_r}{P_n + C + J} \tag{2.11}$$

Where

- C is the clutter.

- J is the interference and jamming.

2.2   Harmonic Radars

The harmonic radar has been developed in the 1980s to rescue avalanche victims [2]. It works by using special skiing shoes which are more visible to the radar than the surrounding environment. Locating the victims can be done by detecting the shoes at two to three meters below the snow. The name comes from the received frequency of the radar which is at the second or third harmonic of the transmitted signal frequency; i.e., two or three times the transmitted frequency. The way to achieve this is by placing a small nonlinear element at the target of interest such as a diode to generate the harmonic frequency and to place an antenna which resonates at both transmit and receive frequencies to allow for proper signal reflections back to the radar receiver. The diode and the antenna placed on the target of interest are called the tag. The tag can be so small and light weight to be placed on a helmet, a life-vest, a skiing shoe, or even on an adhesive tape to be placed on a human body or a small insect. The tag does not require a battery or any source of energy, as it is powered by the transmitted EM wave of the radar. This is an advantage for minimizing the size, weight and maintenance of the tag. Another advantage for this radar is the immunity to clutter since reflections of the surrounding environment will be at the fundamental transmitted frequency, while target reflection is at the harmonic frequency which can be filtered easily using the radar receiver. The radar itself is a regular search and track radar with a transmitter, a receiver and a signal processor. The radar receiver is modified to only detect the harmonic frequency. Due to the clutter immunity, radar transmitter can use lower transmit powers and the receiver can still distinguish small power reflections from the tagged targets. This allows for smaller size, lighter weight and lower cost radar system with no performance degradation. The effect of using harmonic radars on radar parameters are mainly caused by the frequency doubling of the received signal.

- Path loss effect: the return path from targets to the radar system are at double the frequency which affects the path losses as follows:

$$P_L = \left(\frac{4\pi R}{\lambda}\right)^2 \tag{2.12}$$

  It is clear from the above equation, that doubling the frequency increases path losses by four times this translates to 6 dB loss increase in the log-domain.

- Frequency deviation: All frequency deviations caused by Doppler shifts are affected by the frequency doubling due to the tag reflections at the harmonic frequency.

- Target RCS: the tagged target will have a different RCS depending not only on the size and reflectively of the target, but on the tag design and ability to generate the harmonic signal and transmit it back to the radar. The tag can be modeled to estimate the harmonic radar RCS. In this thesis it is assumed that the tag has a reflection loss of around 20 dB, this give a target RCS of [14]:

$$\sigma = 4\pi R^2 \frac{P_{scat}}{P_{inc}} = 4\pi R^2 \cdot 10^{-20/10} \tag{2.13}$$

  Where

  - P_{scat} is the scattered signal power from the tagged target.
  - P_{inc} is the radar incident signal power.

- Radar range equation: the radar received power will be affected by all previous parameters and the radar range equation can be re-written for the harmonic radar as follows:

$$P_r = \frac{P_t G_t G_r \lambda_{TX} \lambda_{RX} \left(4\pi R^2 \frac{P_{scat}}{P_{inc}}\right)}{(4\pi)^3 R^4} \tag{2.14}$$

  Where λ_{TX} and λ_{RX} are the wavelengths of the radar TX and RX signals respectively. More about harmonic radar effects will be covered later in chapter 4.

2.3   Insect Tracking

Harmonic radars are useful for detecting and tracking small targets such as insects since it can distinguish tagged targets from the surrounding environment. It has been used for detecting different types of insects in the ground, over ground or flying such as Beetles, Bees, Moths and other small insects. radars can detect stationary or moving insects and depending on the radar waveform, they can measure targets ranges, radial velocities, azimuth, and elevation angles [6], [13], [10], [7] and [11].

Initial Design and System Parameters

Recent designs for the harmonic radars use high power and low frequency which restricts the size of the tag and the radar transmitter and receiver subsystems, hence limits the portability of the radar and the type of insects to be tagged [13]. Some advancement in reducing the size of the radar has been done in [13], however the system is still too large and heavy to be carried by a drone. In this project a radar system is designed to be lighter and smaller and cover a wider detection range. This is done by investigating the receiver and transmitter designs and possibly using codded radar signals to get some processing gain [15].

3.1 System Requirements

The aim with this Master's thesis work is to design the harmonic radar transmitter, receiver and digitizer subsystems in small size, lightweight and of low power to be carried by a drone in order to track and locate Bogong moth insects around their aestivation sites in the Australian Alps. The radar will use two separate horn antennas for transmitting and receiving initially, however different antennas are designed in another master thesis in 2018 by engineers Ze Fu and Hamza Bin Faheem in [4] to be smaller and lighter and might be used for the final system. Following are general system requirements considered for designing the harmonic radar:

- The frequency of operation for the radar is part of the investigation carried by this thesis, there will be some analysis and comparisons in the next section for different operating frequencies.

- The radar should be battery powered. One battery charge should last for at least one drone flight mission, which is around 50 minutes.

- The radar with the batteries and housing when installed in the drone should weigh less than 2 kg.

- The dimensions of the housing box should be less than 25 cm×25 cm×15 cm.

- The radar should detect tagged Bogong moths in the ranges from 1.5 m to 30 m.

- The radar transmissions should be compliant to the frequency regulations internationally.

To comply with the requirements some investigations have been performed including; frequency of operation, different system configurations, different radar wave-forms and modulations, tag diode simulations, link budget analysis and frequency harmonic analysis.

3.2   Frequency Selection and Regulations

3.2.1   History of Harmonic Radar Frequencies

The idea of using harmonic radars for insect detection has started from 1986 [10] using the same principle of a high-power radar and a tagged insect operating at 915 MHz TX frequency and 1830 MHz RX frequency, the radar is made by Uppsala university to trace ground dwelling insects in the field. As illustrated in the reference paper the radar is huge, carried by the operator in a backpack and the transmitter by his hands, weighting around 15 kg in total. Even if the radar is designed with modern technologies it would be large to be carried by a drone. This is mainly because of the wavelength which effects the antennas, the RF tracks and the tag as well which will be large and disrupt the insect movement.

To make the radar more portable a smaller design is proposed in [13] using higher frequency; C-BAND for transmission at 5.9 GHz and X-BAND for reception at 11.6 GHz, hence use smaller components. The system is designed using connectorized components which makes it large and heavy, however if it is designed using minimum surface mount components it can be small enough to be carried by a drone.

A smaller design at higher frequency X-BAND for transmission at 9.4 GHz and K-BAND for reception at 18.8 GHz is built and tested in [6]. This frequency is the most promising, because of the less number of systems using this band on land and hence less interference; it is mainly used for marine radars and because of the size reduction of the radar system and the tag, however it is a licensed band which requires extra process to acquire the license. The reference paper shows that the system shows good results at short distances up to 1 m [6].

So it is clear that using higher frequency is better for smaller size, lighter weight and portability of the radar system as higher frequency means smaller wavelength, smaller components and PCB tracks. Wavelength also affect the tag size, higher frequency allows for smaller tag antenna, hence smaller and lighter tags which can be placed on smaller insects without compromising their movement.

3.2.2   Path Loss

Different frequency bands have different free space attenuation as shown in Figure 3.1. This can be seen from two different perspectives. First, higher attenuation means higher path losses of the radar and shorter range of operation in limited transmit power applications. Second, higher attenuation means higher transmission losses and less interference of other systems using the same frequency bands.
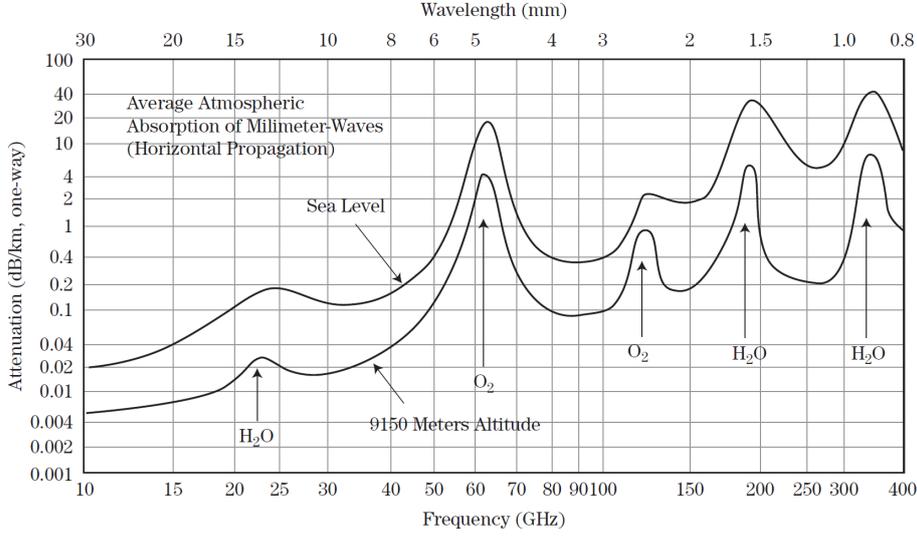
Figure 3.1: Atmospheric Attenuation Over Frequency Bands (From US Government Work) [14].

Since this system is required to be of low operating power (battery powered), it has to have low RF power transmission, then the system should operate in a minimum attenuation frequency band to allow for maximum range of operations. It is clear from the above figure and from (2.7) that as the frequency of operation increases the free-space attenuation increases and the radar received power decrease. However other factors can compensate for these losses i.e. when using fixed aperture antennas, higher frequency means higher antenna gains according to (2.4). This means that the performance will be independent of the frequency if one of the antennas either TX or RX has fixed aperture and the performance will even increase with higher frequency of operation if both antennas have fixed aperture sizes. For the harmonic radar design, one of the antennas is always having a fixed aperture, which is the antenna on the radar side either TX antenna during radar transmission or RX antenna during radar reception. The other antenna which is in the tag is a resonant antenna that is frequency dependent and hence as mentioned before, the size of the tag depend on the frequency of operation, the higher the frequency the smaller the tag which allows for tagging smaller insects. The radar range equation for the harmonic radar will be as follows:

$$P_r = \frac{P_t G_{tag} 4\pi A_e \lambda^2 \sigma}{\lambda^2 (4\pi)^3 R^4} = \frac{P_t G_{tag} A_e \sigma}{(4\pi)^2 R^4} \tag{3.1}$$

3.2.3   Antenna Beam-width

Antenna beam-width changes with frequency, higher frequency gives smaller (narrow) beam-width assuming fixed aperture size. The antenna half power or $3-$dB

beam-width θ_{3dB} can be calculated using the following:

$$\theta_{3dB} = \frac{\alpha\lambda}{D} \ \ rad \ = \frac{180\alpha\lambda}{\pi D} \ \ degrees \qquad (3.2)$$

Where

- $-\alpha$ is the beam-width weighting factor equals to 0.88 if uniformly illuminated.

- $-D$ is the antenna dimension; antenna length if calculating elevation beam-width and antenna width if calculating azimuth beam-width.

When calculated for 915 MHz, 5.8 GHz and 9.41 GHz gives a θ_{3dB} of 110.2°, 17.4° and 10.7°, respectively this give equal power arc lengths at 30 m range of 57.7 m, 9.1 m and 5.6 m respectively. This is shown in Figure 3.2 as well.
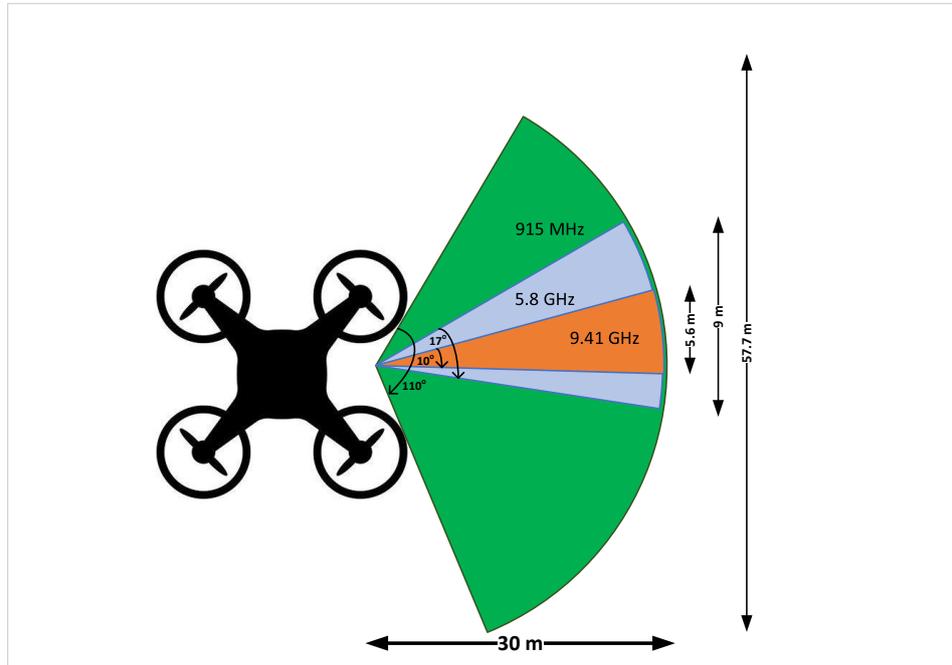
Figure 3.2: Fixed Aperture Antenna Beam-width at Different Frequencies.

3.2.4 Propagation Mechanisms

The wave propagation is frequency dependent as well. Depending on the propagation mechanism, higher frequency can be better or worse, this is dependent on the environment the radar will be working in. As mentioned in Chapter 1, the radar system will be mainly working around the aestivation sites of Bogong moths which are located in caves and crevices underneath rocks and fallen trees. The main propagation mechanisms for the radar wave will be:

- Reflection and Scattering are important for the radar so the signal can propagate inside the caves and reach the tagged moths and propagate back to the radar. As frequency increase the waves are subjected to more specular reflections and less scattering since the objects become larger compared to the signal wavelength. This reduces the chance of signal propagation.

- Diffraction: by rock edges is better at low frequencies since higher frequencies give sharper shadows according to Huygen's principle.

- Transmission or Penetration: propagation is better at lower frequencies according to Friis transmission formula but as mentioned before the aperture gain will compensated for the propagation losses, so it will be independent of frequency.

3.2.5 Licensed and Unlicensed Frequency Bands

When choosing frequency of operation, implementation and regulation challenges must be considered. It is required for this system to be working internationally or at least in two countries, in Sweden and in Australia, to do so frequency regulations of both countries must be considered. This can be done in two different ways:

1. Choosing the frequency of operation in the Licensed Frequency Bands. This means that the frequencies selected for transmission and reception must be available in both countries. The advantages of this approach are:

   - Lower or no interference from other systems using the same frequency, as the frequencies will be entirely dedicated to the operation of the radar, there still can be leakage from nearby frequency channels which can be filtered by the radar receiver.

   - Relaxed transmission power regulations within the frequency of operation compared to the unlicensed transmission regulations, i.e. the system can transmit higher powers.

   However, there are some disadvantages of this approach which can make it very difficult such as:

   - Limitation of frequency bands available around the world. The system might operate at different frequencies in different countries which requires some modifications.

   - Cost of the frequency license which can be very high.

   - Time consuming process of pursuing the license allocation in all required countries, which can be impossible if it is required to operate the radar internationally.

   So after choosing the frequency of operation and applying for the license, the system can not be operational until the license is acquired which can take months or years depending on the importance and the application of the radar.

2. Choosing the frequency of operation in the Unlicensed Frequency Bands. There are a few frequency bands that are available internationally for anyone to use for both transmission and reception with certain regulations for within band and out of band transmissions and for peak and average powers, they are called the Industrial, Scientific and Medical ISM bands. The ISM bands cover different center frequencies from around 7 MHz up to 245 GHz and different bandwidths from 14 KHz up to 2 GHz [1]. The advantages of using the ISM bands are:

   - They are free of charge and available to anyone with no required permissions.
   - Some of the bands are common around the world with similar transmission regulations. So the system can work internationally with no modifications.
   - The system can be operational directly after making sure it complies to the transmission regulations of the ISM bands.
   - Another advantage is the availability and lower cost of electronic components since they are used for different applications and are mass produced.

   However, since the ISM bands are available for everyone, they have large amount of interference especially in crowded areas due to the large number of applications including:

   - Wireless communications including WiFi, Bluetooth, amateur radio, UAV controllers and amateur satellite.
   - Medical equipment.
   - Sensors and radars in vehicles.
   - House items such as microwave ovens, garage openers and wireless modems, etc.

So for interference sensitive applications the first approach is more suitable, given all the limitations of using the licensed bands, but still they are better than having large interference which can disrupt the operation of the system and give false detections.

One way to go around ISM bands interference is if it is possible to prove that there will be minimum interference around the radar operation area, if it is an uninhabited area with less interference in the ISM bands, then the second approach can be used with all of its advantages and with no disturbance on the operation of the radar. The second approach has been considered in this thesis since the radar will be operational around the aestivation sites of the Bogong moths that are outside the cities and in the high altitudes as described earlier in Chapter 1. The 915 MHz and the 5.8 GHz frequencies are in the ISM band, while the 9.41 GHz frequency is in the licensed band, and it is used for marine radar.

The 5.8 GHz TX frequency is considered because it is the highest possible frequency in ISM band for this application, the next TX frequency in the ISM band is at 24 GHz, which is still possible however the RX frequency will be at 48 GHz

which makes the receiver design challenging for the shortage of available components.

For each frequency band there are some transmission regulations set by the license issuer. Even for the unlicensed bands there are some regulations to limit the interference [1]. Figure 3.3 shows an example of transmission regulations at the 5.725 GHz to 5.875 GHz ISM band. The figure shows that the total Effective Isotropic Radiated Power EIRP should be less than 25 mW which is 14 dBm and the out of band transmissions should be less than -40 dBc which is -26 dBm.
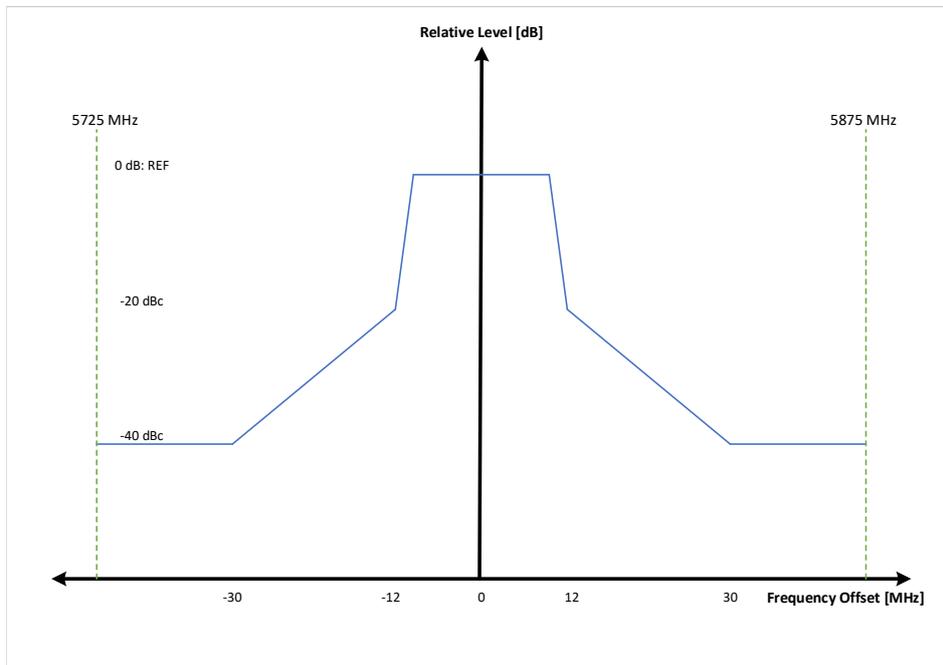
Figure 3.3: Emission Mask for ISM Band. Generated According to
the ISM Standards [1].

3.2.6 Summary

- Choosing the frequency of operation as high as possible to allow for smaller tags and since one of the antennas is always having a fixed aperture, so no increased attenuation with frequency.

- Antenna beam-width decrease with frequency increase for fixed aperture antennas which gives better angle resolution.

- Higher frequency gives better reflections and wave-guiding but lower scattering and diffraction.

- Choosing a frequency in the ISM bands is better due to all of the advantages of ISM bands and because the system is operating in uninhabited locations around Bogong moths aestivation sites.

The rest of this chapter and Chapter 4 will be comparing between 5.8 GHz and 9.41 GHz TX frequencies as they are the most suitable for this application.

3.3 Tag Effects Modeling

The tag is used to highlight the target of interest which is the Bogong moth to the harmonic radar from the surrounding environment. This is done by designing a special antenna with a nonlinear RF element to reflect the radar wave at the second harmonic frequency. The tag design is out of the scope of this thesis, however the effect of the tag on the radar signal is taken into account.
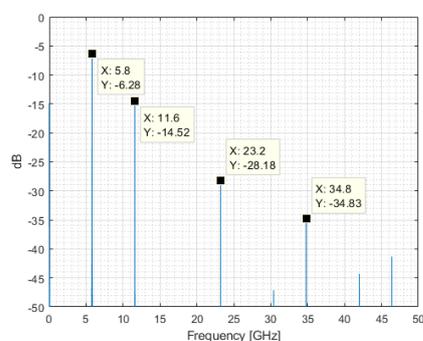
Figure 3.4: Tag Generated Signal in Frequency Domain.
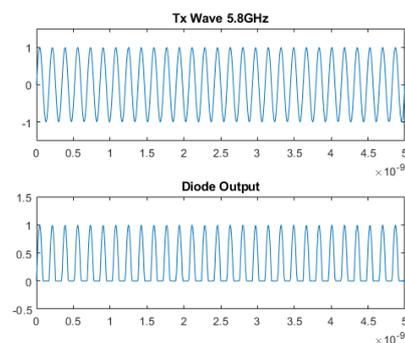
Figure 3.5: Tag Generated Signal in Time Domain.

Figure 3.5 shows the radar TX signal in top plot which is modeled in MATLAB as a sinusoidal signal at 5.8 GHz and tag-diode generated signal in bottom plot, the diode output is zero when the received signal from the radar is below the diode threshold voltage, and it is passing the received signal with some attenuation when it is larger than the threshold voltage. The effect on frequency domain is a generation of multiple signal harmonics as shown in Figure 3.4. These harmonics will be fed to the tag antenna which is a half wave length dipole resonant at the second harmonic frequency 11.6 GHz in this example and the second harmonic signal will be radiated back to the radar. The MATLAB code used for this model is included in Appendix-A.

3.4 System Block Diagram Variants

The main challenges of building this radar system are small size, light weight, low power consumption and very small hidden targets. Different system designs have been considered and compared, the comparisons are covered in the remaining of this chapter and in Chapter 4.
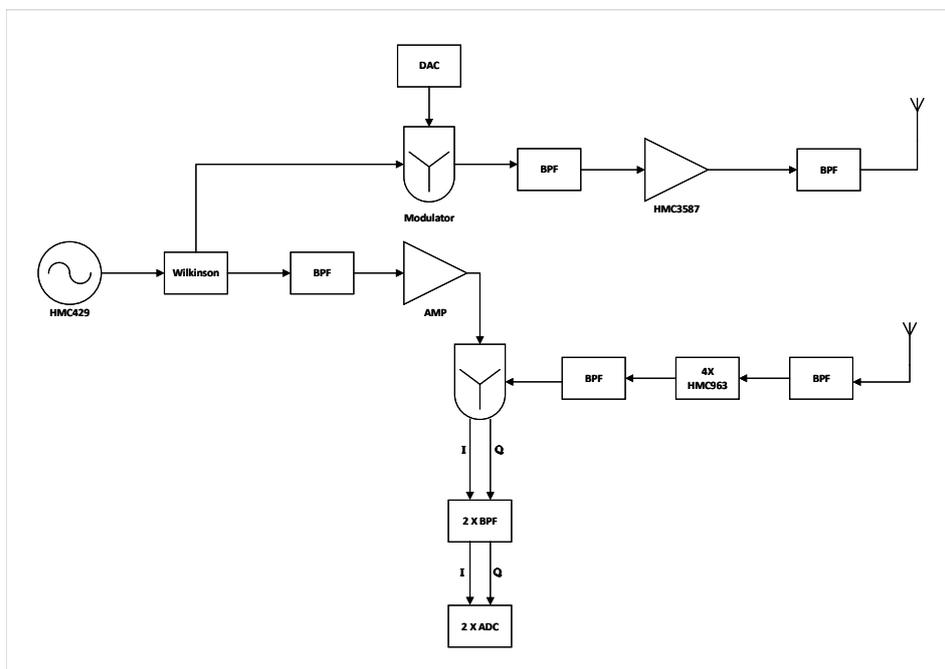
Figure 3.6: Radar System Block Diagram Version 1.

The block diagram in Figure 3.6 shows a simple radar transmitter and receiver sub-systems. The radar transmitter starts by generating the TX carrier signal and its harmonics using the HMC429LP4 Voltage Controlled Oscillator VCO by Analog Devices with output powers of 4 dBm at 5 GHz, −7 dBm at 10 GHz and −19 dBm at 15 GHz. The carrier signal is divided using a simple 2-Way Wilkinson Power Divider to the transmit path to serve as a carrier signal for TX modulation and the receive path to serve as a Local Oscillator LO signal for the receiver down-conversion. A digital base-band signal is converted to analog at 800 MHz using a high speed Digital to Analog Converter DAC and applied to the carrier signal using a double balanced RF mixer. The TX signal is filtered at 5.8 GHz to remove the carrier frequency and other signal Inter-Modulations IMs and then amplified to the required TX power before transmission. The radar receiver receives the signal at twice the TX frequency; 11.6 GHz and often with some additional Doppler effects. The RX signal is filtered and amplified with high amplifications of 60 dB to 80 dB using LNAs to compensate for the path losses with minimum added noise; detailed analysis of link budget and signal and noise powers will be covered in the next section. The RX signal is down-converted using an In-phase, Quadrature-phase Demodulator IQ-DEMOD. The LO used for the demodulation is coupled from the TX carrier signal and filtered at the second harmonic; 10 GHz, then the down-converted IQ signals are at twice the frequency of the base-band TX signal; 1.6 GHz. Two high speed Analog to Digital Converters ADCs are used to convert the IQ signals into digital domain for the radar processor. The choice of base-band frequency at 800 MHz is to make the filtering of TX signal

possible, if lower frequency is selected then filtering the $f_{carrier} + f_{base-band} = 5.8$ GHz TX signal from close IM signals i.e. at $f_{carrier} - f_{base-band}$ will be difficult. It will become challenging if second or third order IM products are considered i.e $f_{carrier} + f_{base-band}$, $f_{carrier} - f_{base-band}$, $f_{carrier} + 2f_{base-band}$ and $f_{carrier} - 2f_{base-band}$. The filtering at the receiver is easier since the IF signals are at twice the frequency of the TX base-band signal.

The disadvantage of this configuration is the use of high speed DAC and ADCs which are power consuming, they also require high processing speeds to handle the data rates, the processor will be power consuming as well and will generate heat while operating which might require a cooling system. These disadvantages effect the size, weight and power consumption of the radar system.
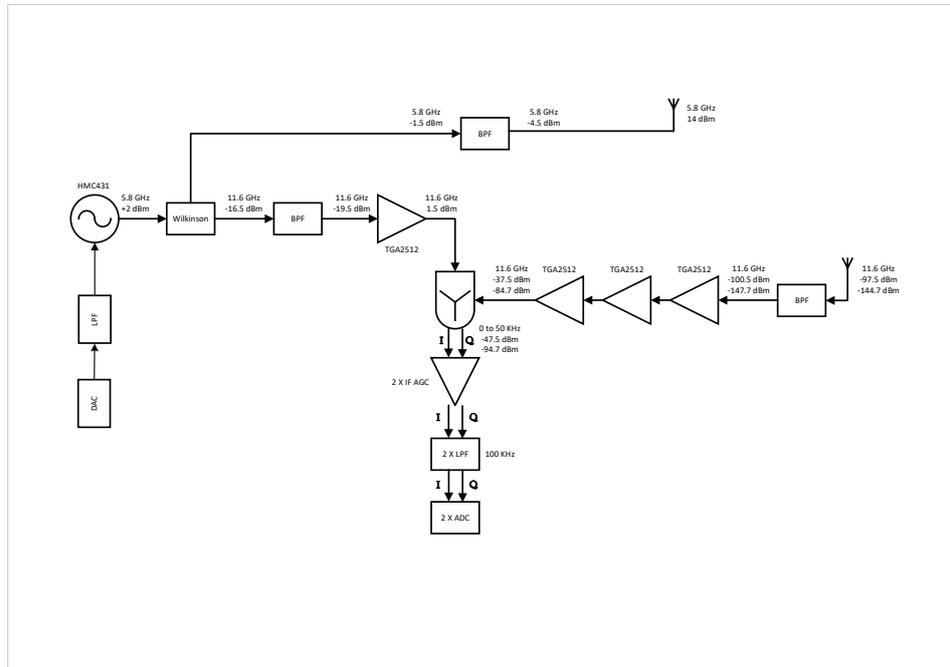
Figure 3.7: Radar System Block Diagram Version 2.

Another system configuration is considered in Figure 3.7 where the VCO used is the HMC431LP4 by Analog Devices which can directly generate the TX signal in the ISM band from 5.725 GHz to 5.875 GHz, it will generate the second and third harmonics as well similar to the first configuration with -15 dBc level for the 2nd harmonic and -30 dBc level for the 3rd harmonic. The VCO is directly modulated by the DAC and out of the modulation is TX signal with harmonics at multiples of the fundamental frequency. There will be no other spurious signals or IM products out of the VCO , so the filtering of TX signal is easier. The TX signal is coupled to the receiver using a 2-Way Wilkinson Power Divider. Three BPFs are used, one in the TX path to select the fundamental frequency component out of the VCO and send it for radar transmission, the second filter is in the coupled path to the receiver sub-system to select the 2nd harmonic frequency and use it

as a LO for the RX signal demodulation and the third filter is used to filter the radar RX signal, it uses the same frequency as the second filter. The RX signal is then amplified using high gain LNAs and demodulated to base-band using an IQ-DEMOD. The base-band IQ signals are filtered and converted to digital domain using two ADCs. The advantages of this configuration are:

- Simple radar transmitter configuration without using a mixer for modulation and not using a transmit amplifier, since the output power of the VCO is sufficient for transmission.

- Less powerful DAC and ADCs used for the base-band signals as the base-band frequency is low compared to the first configuration.

- Less powerful processor required to handle the digital data.

- Small size, light weight and less power consumption.

However, there are some disadvantages as well that limit the operation of the radar when using this configuration. First, the limitation of modulation techniques; only frequency modulation can be used with this configuration. Second, is the frequency inaccuracy and non-linearity of frequency sweeps of the free running VCO with no phase locking. This causes changing frequency in the receiver base-band signals.
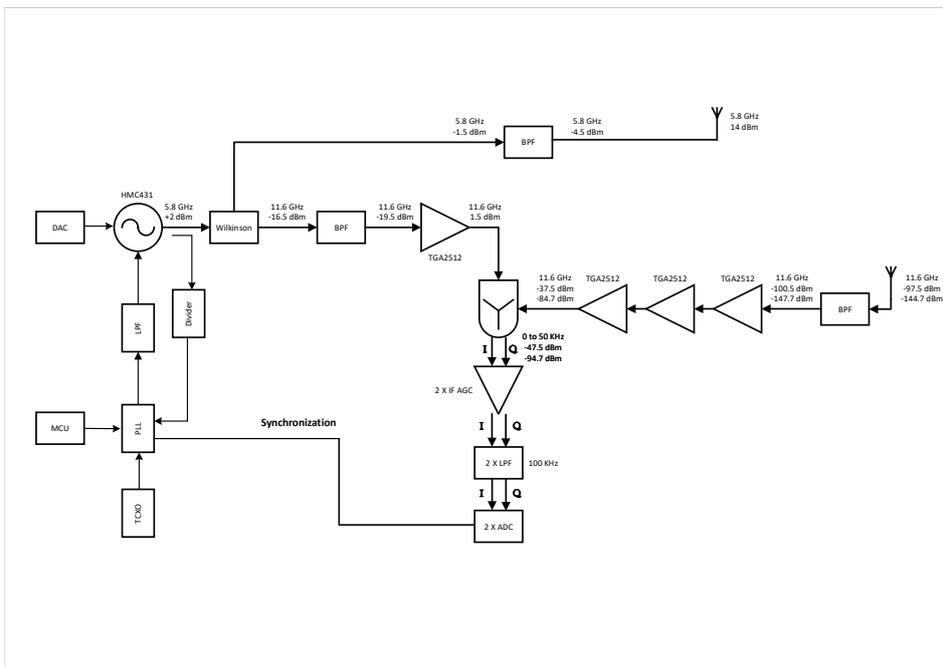
**Figure 3.8:** Radar System Block Diagram Version 3.

The third system configuration considered is shown in Figure 3.8. This configuration is similar to the second configuration with some changes in the generation

of TX signal. A Phase Locked Loop PLL is used to generate the VCO tuning volt-
age accurately and compare it to a reference crystal oscillator. The PLL works
by comparing a coupled signal from the VCO output with a clean Temperature
compensated Crystal Oscillator reference TCXO and make sure they are locked at
the same phase. If the phase is different an output current is generated out of the
PLL charge pump and filtered using the loop LPF to give the VCO tuning voltage
[3]. The PLL uses a frequency divider to divide the VCO output frequency since
it is much higher than the TCXO reference frequency. The output of the VCO is
coupled to the PLL using a simple Directional-Coupler. A Micro-Controller MCU
is used to control the PLL divider and select the required modulation technique.
The advantages of this configuration include all the advantages of the second con-
figuration in addition to:

- Accurate frequency output and linear frequency sweeps.

- The ability to do frequency and phase modulations using the PLL.

- Lower TX signal phase noise and lower spurious emissions.

3.5   Link Budget Analysis Comparisons

Link budget analysis is performed to make sure that the system with all selected
components will operate as required, this is done by calculating the received power
P_r and the noise power P_n at all stages and make sure that the SNR at the final
stage of the radar receiver is still above a requirement threshold derived from
the system requirements. Figure 3.10 shows a simple link budget analysis at
two different frequencies. The first step is to convert all signal powers, noise
powers, gains and losses to log-domain where, $P_{dB} = 10 \cdot log_{10}(P_{linear})$. Then, all
multiplications and divisions in linear-domain become additions and subtractions
respectively in log-domain. The radar range equation (2.7) becomes:

$$P_{r|dBm} = P_{t|dBm} + G_{t|dB} + G_{r|dB} + 20 \cdot log_{10}(\lambda) + 10 \cdot log_{10}(\sigma) - 30 \cdot log_{10}(4\pi) - 40 \cdot log_{10}(R) \qquad (3.3)$$

And the receiver noise power in (2.8) becomes:

$$P_{n|dBm} = 10 \cdot log_{10}(k) + 10 \cdot log_{10}(T_0) + NF + 10 \cdot log_{10}(B) + 30dB \qquad (3.4)$$

Where, $NF = 10 \cdot log_{10}(F)$ is the receiver noise figure and the addition of 30 dB
is to convert from dBW to dBm. The receiver SNR in (2.9) becomes:

$$SNR_{dB} = P_{r|dBm} - P_{n|dBm} \qquad (3.5)$$

The system used for calculating the link budget in Figure 3.10 uses the third
system configuration described in the previous section in Figure 3.8. According
to the ISM standard specifications mentioned in [1], the total EIRP should be
less than 25 mW, that is the $P_t \cdot G_t$; transmit power after the multiplication with
transmit antenna gain. The TX antenna used is a 15 cm×15 cm rectangular
aperture antenna with antenna gains of 18.5 dB and 22.5 dB at 5.8 GHz and 9.41
GHz transmit frequencies respectively, where the antenna gain is calculated using

(2.4) assuming aperture efficiency $\eta = 0.65$. The TX power regulation at the marine band at 9.41 GHz is higher than 25 mW, but considering equal transmit powers P_t for both systems for fair comparisons, and given that TX antenna gain at 9.41 GHz is higher, then EIRP of the 9.41 GHz system is higher as shown in Figure 3.10. Path losses of each system are calculated for both directions; radar TX direction and radar RX direction. Assuming Line of Sight LoS radar signal to the target and maximum radar range of 30 m, path loss P_{LdB} is calculated using Friis transmission formula as follows:

$$P_{LdB} = 20 \cdot log_{10}(\frac{4\pi R}{\lambda}) \tag{3.6}$$
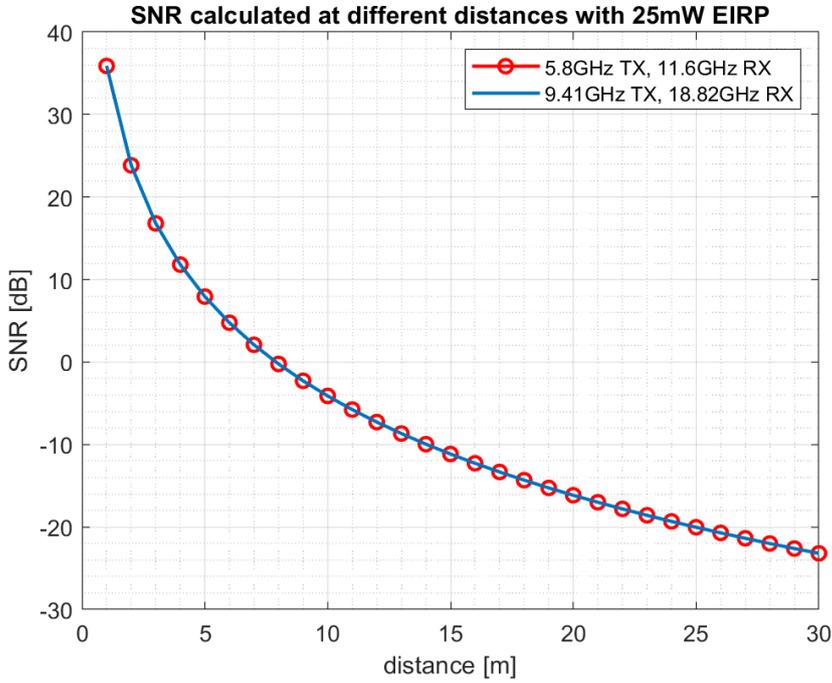
Figure 3.9: SNR of Radar Signal Vs. Range at Different Frequency of Operation.

It is clear from the P_L equation and as shown in the link budget diagram that losses increase with frequency increase. The tag reflection is considered in worst case scenarios to be -20 dB for both systems, however investigations about the tag should be made in a separate project to support the proper functionality of the radar. Since the reflected signals from the tag are at twice the frequency of the radar TX signals, they are subjected to more path losses; $20 \cdot log_{10}(2\times) = 6$ dB loss increase. RX antenna gains are frequency dependent as well, the radar receiver is using a similar 15 cm×15 cm rectangular aperture antenna with antenna gains of 24.5 dB and 28.5 dB at 11.6 GHz and 18.82 GHz receive frequencies
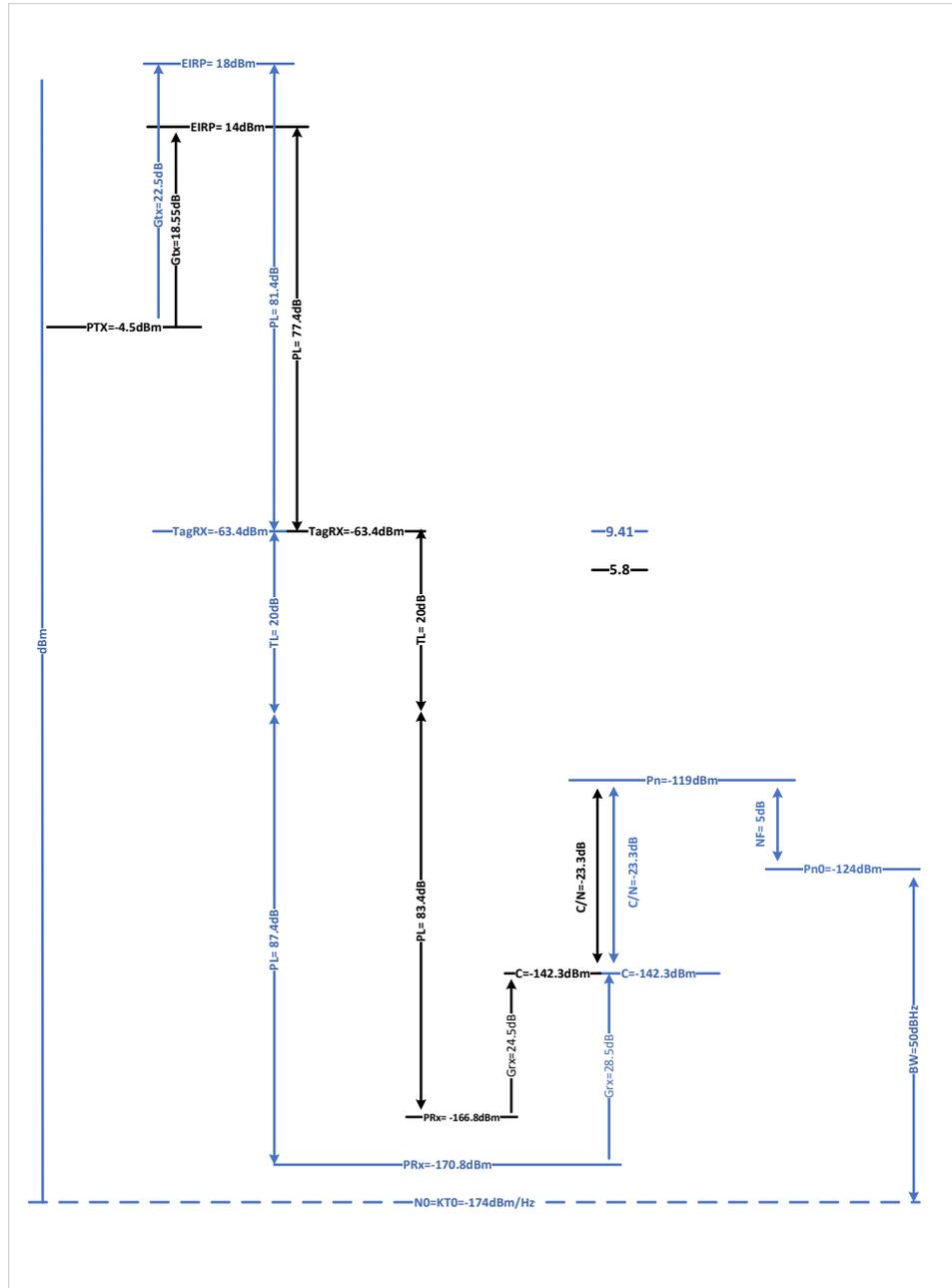
Figure 3.10: Link Budget Analysis at Different Frequencies.

respectively. The receiver noise power is bandwidth dependent according to (2.8), in the calculation of this simple link budget, the radar receiver noise bandwidth is determined by the bandwidth of the final filtering stage of the radar receiver before IF signal digitization [12]. The system NF affects the noise power, as shown in the link budget diagram. This diagram shows that at 30 m range the SNR of the system will be negative which means the signal power will be below noise power. To solve this issue without increasing the TX power or antenna gains, processing gain should be included using modulation. This will be discussed in Chapter 4, detailed analysis of the system link budget including processing gains will be covered in Chapter 5. A MATLAB model for link budget analysis at both frequency bands and for ranges from 1.5 m to 30 m is included in Appendix-A. The simulation results of the model is shown in Figure 3.9.

Radar Waveform Design

It has been shown in the previous chapter that transmitting a simple non-modulated radar signal is not sufficient for this application. It is required to use some correlation between the known transmit signal and the received signal from target reflections in order to extract the weak signal out of the high receiver noise. In order to achieve correlation gain at the receiver, proper radar waveform should be designed taking into account the required correlation gain and all other system requirements. Radar wave-forms can be categorized into two different categories: Pulsed wave radars and Continuous Wave radars CW.

4.1 Pulsed Radar

A pulsed radar is transmitting signals only during the pulse transmission period or pulse width τ, during this period the receiver is OFF to avoid false alarms and to protect receiver components from high power leakage. The radar receiver is active just after the pulse duration, the time the receiver is active is called echo or listening duration. The sum of both durations is called the radar Pulse Repetition Interval PRI. This interval keeps repeating during the operation of the radar, sequencing between the TX and RX times. The Pulse Repetition Frequency PRF is another parameter of pulsed radar related to PRI as follows:

$$PRF = \frac{1}{PRI} \tag{4.1}$$

The Duty Factor, Cycle or Ratio D_R is the ratio between TX time and total period time calculated as follows:

$$D_R = \frac{\tau}{PRI} = \tau \cdot PRF \tag{4.2}$$

This is a useful parameter to calculate the average transmit power of the pulsed radar P_{avg}

$$P_{avg} = P_t \cdot D_R = P_t \cdot \tau \cdot PRF \tag{4.3}$$

Where P_t is the peak RF transmit power. The radar range equation (2.7) has to be modified to include P_{avg}. The pulsed radar range equation becomes:

$$P_r = \frac{P_{avg}G_tG_r\lambda^2\sigma}{(4\pi)^3 R^4} \tag{4.4}$$
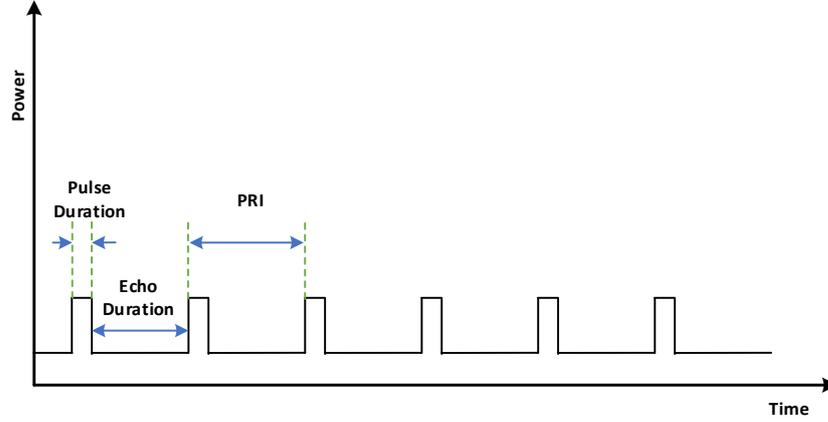
Figure 4.1: Pulsed Radar Waveform.

Figure 4.1 shows the pulsed radar waveform in time domain with definitions of all duration parameters mentioned above.

4.1.1 Range Measurement and Range Resolution

Range measurement using pulsed radars can be done by calculating round-trip time ΔT of the reflected radar signal from the target as shown in (2.1). Since the receiver is only active during the listening duration, it can not receive the reflections from very close targets with ΔT inside the transmission period τ, this sets the minimum detection range of the pulsed radar to:

$$R_{min} = \frac{c\tau}{2} \tag{4.5}$$

The undetectable range below R_{min} is known as blind range of the radar. It depends on the radar pulse width τ, so selecting τ is a compromise between higher average power and minimum detection range.
Range resolution is another radar parameter that depends on the selection of τ, the range resolution ΔR is the ability to distinguish between closely spaced targets. For the non-modulated pulsed radar wave-form, range resolution is

$$\Delta R = R_{min} = \frac{c\tau}{2} \tag{4.6}$$

So the radar can resolve targets that are separated by at least ΔR. Targets which are separated by less than ΔR will be detected as a single target regardless of their numbers and reflected powers. Also a target which is large enough to cover more than ΔR will be detected as multiple targets. The total radar range is resolved into range steps called range bins or gates separated by ΔR.
The radar maximum range R_{max} is a function of the PRI and can be found as

following

$$R_{max} = \frac{c \cdot PRI}{2} = \frac{c}{2 \cdot PRF} \tag{4.7}$$

This range is called the maximum unambiguous range of the radar as it can be resolved within one PRI, if a target is detected beyond R_{max} then it is considered in the next PRI and the range is ambiguous. To avoid range ambiguities PRI can be chosen large enough to cover the furthest required targets.

$$PRI_{min} \geq \frac{2R_{max}}{c} \tag{4.8}$$

4.1.2   Velocity Measurement

Velocity measurements for a pulsed radar is done by measuring the relative motion between the radar and the target using Doppler effect as mentioned in (2.2). The Doppler frequency generated from target movement is sampled at the radar PRF. The maximum Doppler shift for a given PRF according to Nyquist sampling theorem is

$$f_{dmax} = \pm \frac{PRF}{2} \tag{4.9}$$

For Doppler shifts larger than f_{dmax} the velocity of the target is unambiguous and to resolve such velocities the radar PRF must be increased to at least PRF_{min} and hence the radar maximum unambiguous range R_{max} is compromised according to (4.7).

$$PRF_{min} \geq 2f_{dmax} \tag{4.10}$$

The maximum unambiguous target velocity according to (2.2), (4.9) and (4.10) is

$$v_{max} = \lambda \frac{f_{dmax}}{2} = \pm \lambda \frac{PRF}{4} \tag{4.11}$$

So selecting the radar PRF is a compromise between the maximum unambiguous range and maximum unambiguous velocity measurements of the radar.

4.1.3   Processing Gain

As shown in the simple link budget analysis in Chapter 3, the received SNR at the maximum range and LOS conditions is below -24 dB, however this was calculated for a receiver bandwidth of only 100 KHz. If the bandwidth is increased, the receiver noise power increases and the SNR decreases further below -24 dB. Another factor is the propagation condition, the calculations were made for a LOS condition which has a path loss exponent of 2. If other conditions apply, path loss exponent increase and path losses increase exponentially, then radar received power decreases and SNR decreases. This requires a high processing gain of at least 30 dB to 50 dB to make sure that the system will perform as required. Pulse integration and pulse compression are two receiver techniques used in pulsed radars to improve the SNR and range resolution.

Pulse Integration

Pulse integration works by transmitting multiple pulses on a target of interest and integrating all signal returns to improve received signal power while receiver noise power is unchanged. Ideally the improvement is a multiplication by the number of pulses transmitted assuming the radar, the target and the environment are fixed and the radar antennas are pointing toward the target the whole time during transmission and reception of all pulses; this is known as Coherent Pulse Integration:

$$SNR_c(N) = N \cdot SNR(1) \tag{4.12}$$

Where

- N is the number of transmitted radar pulses.

- $SNR_c(N)$ is the coherently integrated SNR of N pulses.

- $SNR(1)$ is the SNR of one pulse calculated from (2.9).

However if the radar, the environment or the target are moving, the phase of the received signal will change (phase rotation) and this will effect the integration of the received pulses. If two pulses are out of phase then the addition goes to zero. To overcome this issue, non-coherent pulse integration is often used, by integrating the signals amplitudes and discarding the phases. Then the non-coherently integrated SNR of N transmitted pulses is

$$SNR_{nc}(N) = \sqrt{N} \cdot SNR(1) \tag{4.13}$$

Dwell time T_d is the time required for the radar to transmit and receive all the N pulses

$$T_d = N \cdot PRI \tag{4.14}$$

In order to achieve the require 30 dB of processing gain to improve the received SNR using non-coherent pulse integration, it is required to transmit at least one million pulses and integrate them according to equation (4.13). This requires a dwell time on target of at least 200 ms for a maximum target range of 30 m according to equations (4.7) and (4.14).

Pulse Compression

As mentioned before range resolution for non-modulated pulsed radar is a function of transmitted pulse width τ. Radar transmitted energy and average power P_{avg} are functions of τ as well, so if a better resolution is required, τ should be set smaller, then the transmitted energy and P_{avg} of the radar are smaller which affects the ability to detect small and long range targets. Range resolution is dependent on signal Bandwidth B, for a simple non-modulated pulse the Nyquist double sided bandwidth B and range resolution ΔR in terms of signal bandwidth are [14], [9]:

$$B = 1/\tau \Rightarrow \Delta R = \frac{c}{2B} \tag{4.15}$$

To improve radar range resolution ΔR without changing τ or P_{avg}, the signal bandwidth must increase and to increase the bandwidth without changing the

pulse duration, modulation within the pulse is used, this is called pulse compression. It works by keeping the pulse width fixed and modulating the signal within the pulse in the radar transmitter, then matching the received radar signal to the transmitted modulated pulse. Pulse compression is also used for improving the SNR without changing the transmit EIRP. The improvement on SNR after pulse compression is a time-bandwidth τB product by the SNR of the non-modulated pulse.

$$SNR_{Cmp} = SNR_{nm} \cdot \tau B \qquad (4.16)$$

Where SNR_{Cmp} and SNR_{nm} are the received SNR after pulse compression and before pulse compression respectively.

4.1.4   Modulation Techniques

The radar pulse can be phase or frequency modulated to increase the signal bandwidth, in order to improve the radar range resolution and improve the SNR as discussed in pulse compression section.

Phase-Modulated Waveforms

The pulse is divided into small sub-pulses called chips by varying the phase of each chip with a certain code. The code is fixed and is used in the receiver as a matched filter. Ideally the range resolution of the coded pulse is dependent on the chip width τ_{chip} which is much smaller than the pulse width.

$$\Delta R = \frac{c\tau_{chip}}{2}, \ \ B_{chip} = 1/\tau_{chip} \qquad (4.17)$$

Where B_{chip} is the new signal bandwidth after phase modulation. Also the chip duration can be calculated from the pulse duration τ and the number of chips per pulse N_{chips} as

$$\tau_{chip} = \frac{\tau}{N_{chips}} \qquad (4.18)$$

As mentioned before the SNR improvement after pulse compression is a time-bandwidth product. For the phase modulated radar pulse the received SNR is improved as

$$SNR_{Cmp} = SNR_{nm} \cdot \tau B_{chip} = SNR_{nm}\frac{\tau}{\tau_{chip}} = SNR_{nm} \cdot N_{chips} \qquad (4.19)$$

There are different phase coding techniques that can be used for radar waveforms, one of the most common is the Bi-phase Codes such as Barker codes which will be investigated for this design.

Barker Codes

Bi-phase codes use {0°, 180°} phase shifts between signal alternatives represented by baseband code elements of {1, -1} respectively. These codes are easy to implement and they provide good side-lobe reduction after compression (Match Filter).

Peak side-lobe to main-lobe power ratio of Barker codes of length N_{chips} is expressed as

$$S_{LL} = 20 \cdot log_{10}(1/N_{chips}) \tag{4.20}$$

Where S_{LL} is the peak side-lobe power level normalized to main-lobe and measured in dBc. The shortest Barker code has a length of 2 and the longest has a length of 13, they have main to side-lobe ratios as shown in Table 4.1 [14].

Length	Sequence	Main to Side-lobe Ratio [dB]
2	{1, -1} or {1, 1}	-6.0
3	{1, 1, -1}	-9.5
4	{1, 1, -1, 1} or {1, 1, 1, -1}	-12.0
5	{1, 1, 1, -1, 1}	-14.0
7	{1, 1, 1, -1, -1, 1, -1}	-16.9
11	{1, 1, 1, -1, -1, -1, 1, -1, -1, 1, -1}	-20.8
13	{1, 1, 1, 1, 1, -1, -1, 1, 1, -1, 1, -1, 1}	-22.3

Table 4.1: List of Barker Codes [14].

There are available longer phase codes such as Minimum Peak Side-lobe (MPS) codes of lengths up to 40 and Poly-phase Barker codes of lengths up to 63. But for simplicity bi-phase Barker codes are considered in this design.

Barker Code Waveform Design

It is required to design a radar waveform to achieve the system requirements mentioned in Chapter 3. The radar waveform affects some of the radar system specifications. The most relevant specifications include the following:

1. $\tau \leq 10$ ns: to cover a minimum radar range of 1.5 m, the pulse width should be less than or equal to 10 ns according to equation (4.5).

2. $B \geq 1.3$ GHz: as a consequence of choosing a small pulse width and a long Barker sequence to improve the SNR, the system bandwidth increase to at least 1.3 GHz according to equation (4.17).

3. $PRI \geq 200$ ns: to cover a maximum unambiguous range of 30 m, the PRI should be more than or equal to 200 ns according to equation (4.8).

A MATLAB model has been generated to simulate the Barker code waveform and study the design parameters, the code for the MATLAB model is included in Appendix-A. Figure 4.2 shows a Barker code sequence of length 13 in the top plot and modulated at a chip rate R_{chip} of 100 Mbps in the bottom plot. The plot shows the chip duration τ_{chip} to be 10 ns and the pulse duration τ is 130 ns which is 13 times the chip width and the radar minimum range is affected, to solve this higher modulation rate is required.

Figure 4.3 shows the correlation gain output of the matched filter receiver for a Barker sequence of length 13. It is shown that in Barker codes the side-lobe peaks are all equal and the ratio between main-lobe and side lobes are as shown in (4.20).
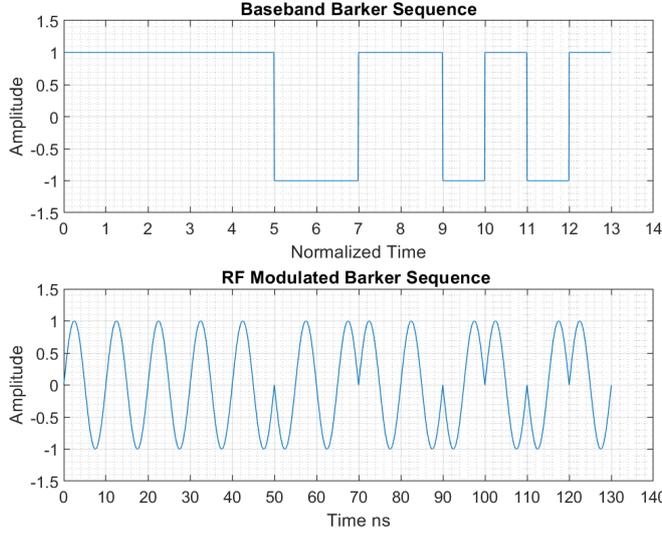
Figure 4.2: Barker Sequence of Length 13.

So in this example the range resolution is 13 times better since the correlation peak shown in Figure 4.3 has a width of one τ_{chip} after pulse compression. However, the range resolution improvement by increasing the pulse bandwidth does not improve the the radar minimum range, it is still calculated using the full pulse width τ as shown in (4.5). To improve R_{min} the transmit pulse width τ still need to be chosen smaller which affects the code rate of the modulation. The pulse width to detect $R_{min} = 1.5m$ should be less than 10 ns. Then if 13 chips Barker code modulation is chosen, the chip duration is 0.77 ns. This requires a code rate of at least 1.3 Gbps to perform the modulation.

Figure 4.4 shows a comparison in time domain between a CW radar signal, a pulsed radar signal and a modulated pulsed radar signal with Barker code of length 13. The pulsed and the modulated pulsed use a pulse width of 10 ns as specified to cover the radar minimum range, note that the figure shows only part of the PRI to make things visible, The PRI as specified is 200 ns to cover the maximum range of the radar.

Figure 4.5 shows the frequency response of the CW radar signal, the pulsed radar signal and the modulated pulsed radar signal with Barker code of length 13. It is shown in the figure that the bandwidth of the pulsed radar signal is wide, approximated by equation (4.15) to be 100 MHz. The bandwidth of the Barker code modulated signal is 13 times larger according to (4.17) which is around 1.3 GHz as shown in the figure as well in order to keep the radar minimum range unchanged.
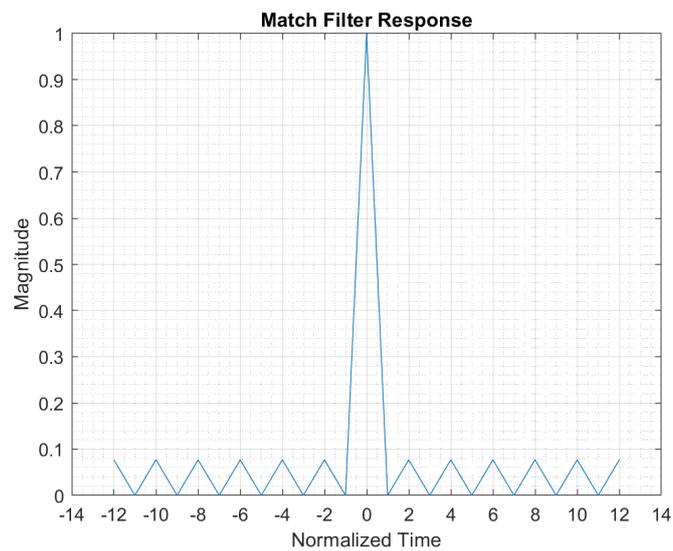
Figure 4.3: Barker Sequence Match Filter Correlation Gain.
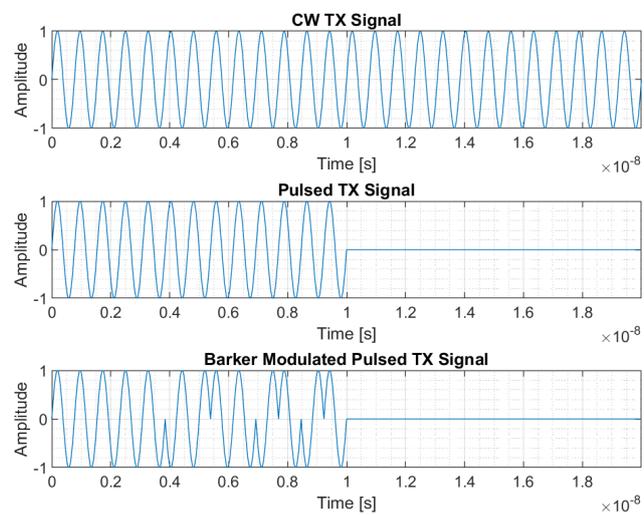
Figure 4.4: Comparisons of Radar Waveforms: CW, Pulsed Non-modulated and Pulsed Barker Code Modulated in Time Domain.
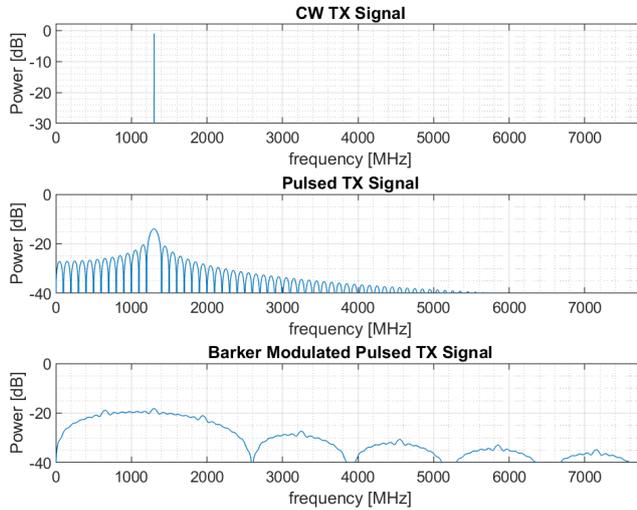
Figure 4.5: Comparisons of Radar Waveforms: CW, Pulsed Non-
modulated and Pulsed Barker Code Modulated in Frequency
Domain.

Frequency-Modulation Waveforms

In frequency modulated pulsed waveforms the modulation is done by changing
the signal frequency within the pulse. The simplest form of frequency modulated
waveforms is Linear Frequency Modulated LFM waveform, where the frequency of
the signal changes linearly with time. This technique has been used since the 1950s,
it is much easier to implement and provide some Doppler tolerance. The frequency
sweeps over a bandwidth B which is selected to provide the required compression
gain. The compression gain is still a time-bandwidth product, however the sidelobe
levels of the compressed waveform are higher compared to the phase modulated
waveform. Sidelobe level can be reduced using weighting functions such as Taylor
weighting function. This technique was not studied thoroughly and was not tested
since phase modulation analysis was enough to get a proper comparison between
pulsed and CW radar waveforms.

Summary of Pulsed Waveform

Using pulsed waveform has the advantage of isolation between radar transmitter
and receiver especially in small size radars where the physical separation between
the transmitter and receiver are limited, however there are some disadvantages in
using pulsed waveform including:

- Limitation of transmit energy since the transmitter is active only in a small
  time period.

- Increased bandwidth and data rate since the minimum range of the pulsed radar limits the maximum pulse width and this sets the minimum non-modulated bandwidth as shown in (4.5) and (4.15). Note that this bandwidth will further increase if modulation is used as shown in section (4.1.4).

- Increased processing requirement. Since the data rates are high, the radar needs high speed DAC, ADCs and processors. This affects the cost, the power consumption and the size of the radar system.

4.2   Continuous Wave Radar

A CW radar is continuously transmitting and continuously receiving, This requires proper isolation between the radar transmitter and receiver subsystems to avoid transmit leakage into the receiver and false alarms. Since the radar is always transmitting, the transmit duty ratio is 100% and the average transmit power equals to the peak RF power.

$$P_{avg} = P_t \cdot D_R = P_t \tag{4.21}$$

The radar range equation for received power, the noise power and the receiver SNR are calculated using (2.7), (2.8) and (2.9). Range measurements in non-modulated CW radars are ambiguous since target returns cannot be referenced to transmit signal times and hence signal round trip times cannot be calculated, so it is not suitable for range measurements. The main use of this radar is for velocity measurement which can be done by measuring the Doppler shifts on the reflected signals using (2.2), so velocity measurements are unambiguous for non-modulated CW radars. For the CW radar to measure range it has to change the transmitted wave so it can identify the signal returns. One of the most commonly used techniques is the Frequency Modulated Continuous Wave (FMCW) radars.

FMCW Radar

FMCW radar generates a frequency modulated CW signal and use it for radar transmission. The modulation is done by continuously sweeping the transmit frequency over a frequency range called sweep frequency, f_{sweep}. The transmitter should complete a full f_{sweep} during one sweep duration, T_{sweep}. The radar receiver compares the reflected target signal with the currently transmitted radar signal and generates a difference frequency called beat frequency, f_{beat}. The simplest form of FMCW waveforms is using LFM, when the frequency changes linearly with time, this is called the chirp waveform. The name chirp comes from bird sounds since the early chirp radars use audio receivers and the radar operator listens to the chirping sound of the baseband received signal. For a FMCW transmitter that sweeps over a frequency range of B, the transmit frequency sweeps can be ascending from 0 to B which is called up-chirp or descending from B to 0 which is called down-chirp, both are called sawtooth chirps as shown in the top part of Figure 4.6. Another technique which is helpful for measuring both range and velocity is to use ascending and descending chirps from 0 up to $\frac{B}{2}$ then from $\frac{B}{2}$ back to 0. The technique is called triangular chirp waveform as shown in the

bottom part of Figure 4.6. But since in this project we are only interested in range measurements, we will continue using sawtooth chirp waveforms.
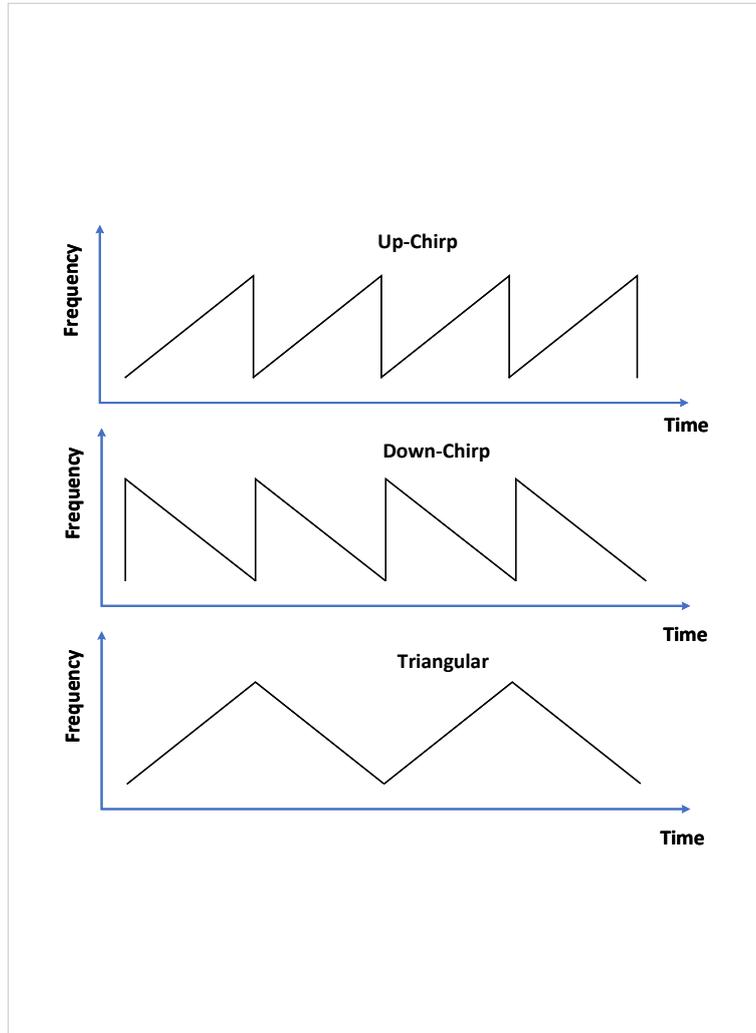
Figure 4.6: Up-Chirp, Down-Chirp and Triangular LFM Waveforms.

Range Measurement and Range Resolution

The FMCW radar uses beat frequency of the reflected target signals compared to the currently transmitted radar signal to estimate the targets ranges. The range also depends on the slope of the chirp transmitted S, where the slope is calculated using the following equation:

$$S = \frac{f_{sweep}}{T_{sweep}} \tag{4.22}$$

Where

- S is the slope of the transmitted chirp signal.

- f_{sweep} is the full range of frequency sweep.

- T_{sweep} is the time it takes to complete a full frequency sweep.

The round-trip time ΔT of the reflected signal from the target can be calculated from the measure beat frequency and the slope of the transmitted chirp as follows:

$$\Delta T = \frac{f_{beat}}{S} \qquad (4.23)$$

The target range can be calculated using the slope of the chirp and the beat frequency as follows:

$$R = \frac{\Delta T \cdot c}{2} = \frac{f_{beat} \cdot c}{2 \cdot S} \qquad (4.24)$$

The range resolution of the FMCW radar is similar to the pulsed radar. It can be calculated from the modulation bandwidth of the transmitted signal. In the FMCW radar, the modulation bandwidth equals to the sweep frequency and the range resolution can be calculated as follows:

$$\Delta R = \frac{c}{2B} = \frac{c}{2f_{sweep}} \qquad (4.25)$$

The FMCW radar minimum range R_{min} is ideally zero if the receiver is able to detect tiny frequency drifts. However in practical systems, receivers can detect small frequencies down to a limit set by the receiver DC blocking components that are used to protect the receiver's sensitive components from high DC voltages. This gives an improvement over the pulsed radar since the minimum range is independent of the system bandwidth.

The FMCW maximum range R_{max} depends on the chirp signal sweep time T_{sweep}. To detect further target T_{sweep} must be increased to be larger than the round-trip time of the reflected signal from the furthest target ΔT.

FMCW Waveform Design

In this project it is required to design a waveform to detect targets from 1.5 m up to 30 m. To do so a chirp sweep time T_{sweep} has to be selected to at least cover the 30 m target round-trip duration.

$$T_{sweep} \geq \Delta T_{max} = \frac{2R_{max}}{c} = \frac{2 \times 30}{3 \times 10^8} = 200 \times 10^{-9}s \qquad (4.26)$$

The sweep frequency f_{sweep} of the chirp waveform is selected to achieve the required range resolution of the radar. For this application, it is required to detect the moths with no strict requirement for the range resolution. For illustration a 50 MHz sweep bandwidth gives a range resolution of:

$$\Delta R = \frac{c}{2B} = \frac{3 \times 10^8}{2 \cdot 50 \times 10^6} = 3m \qquad (4.27)$$

A range resolution of 3 m is enough for the application, also it is manageable within the ISM band between 5.725 GHz and 5.875 GHz.

For the FMCW radar designed it is required to generate a f_{sweep} of 50 MHz starting from 5.8 GHz up to 5.85 GHz to be inside the ISM band with a safe margin and the sweep should be performed in a T_{sweep} of 1 ms to get acceptable level of f_{beat}, for a given range and fixed f_{sweep} higher T_{sweep} produce lower f_{beat} and lower T_{sweep} produce higher f_{beat} acoording to (4.23). The radar range should be as specified between 1.5 m to 30 m. This corresponds to a f_{beat} as follows:

$$\frac{f_{sweep} \cdot \Delta T_{min}}{T_{sweep}} \leq f_{beat} \leq \frac{f_{sweep} \cdot \Delta T_{max}}{T_{sweep}} \tag{4.28}$$

$$\frac{50 \times 10^6 \cdot 10 \times 10^{-9}}{1 \times 10^{-3}} \leq f_{beat} \leq \frac{50 \times 10^6 \cdot 200 \times 10^{-9}}{1 \times 10^{-3}} \tag{4.29}$$

$$500 Hz \leq f_{beat} \leq 10 KHz \tag{4.30}$$

But since we are designing a harmonic radar, the f_{beat} at the receiver will have a doubling effect caused by the tag frequency doubling effect. Hence the f_{beat} for harmonic radar should be twice the normal radar f_{beat} and should range between $1 KHz \leq f_{beat} \leq 20 KHz$. This range of frequencies can be sampled and digitized with a low cost small ADC component, this is a requirement to keep size and power consumption as low as possible.

Processing Gain

Processing gain of the FMCW radar depends on the number of points to perform the FFT at the radar receiver [16]. Since the FFT processor is averaging the amplitude squared of the total number of samples of the received signal, hence more number of samples gives more processing gain. The number of FFT samples depends on the sampling rate of the radar receiver ADC. The radar requires at least 30 dB of processing gain to get positive SNR. Assuming coherent signal integration and assuming all beat frequencies fall directly on FFT bins [16], 30 dB of processing gain requires at least a thousand integration sweeps within detection time of the radar while the drone is moving at maximum speed. The selected drone is the DJI S1000 spreading wings which travels at a maximum speed of 60 Km/h or around 17 m/s, detailed analysis of this is covered the radar processor design in chapter 5.

Detailed System Design and Simulations

5.1 Proposed System Specifications

According to the system requirements and to the history of the harmonic radars and the investigations made in this thesis, the proposed system specifications are as shown in Table 5.1.

Parameter	Specification	Unit	Description
Center Frequency	$5.725 \leq f_c \leq 5.875$	GHz	Choosing this frequency is better since it is the highest possible frequency in ISM band as investigated in Section 3.2.5
Instantaneous Bandwidth IBW	≤ 150	MHz	The full operational bandwidth should be less than 150 MHz according to the ISM standard [1].
Bandwidth	50	MHz	Bandwidth of the radar is dependent on the radar range resolution for pulsed radars an on the delay-bandwidth product for the FMCW radars, as discussed in the waveform design in Chapter 4. It should also be within the ISM band with a considerable margin to avoid out of band transmissions.

EIRP	25	mW	The effective radiated power should be less than 25 mW, that is the transmitted power after the gain of the TX antenna. This is according to the ISM transmission regulations [1].
TX antenna Gain	20	dBi	This is the gain of the final product antenna which is a passive patch antenna array of size 20 cm × 20 cm as proposed in [4]. The TX antenna used for testing is a standard rectangular horn antenna with a gain of TBD.
RX antenna Gain	26	dBi	This is the gain of the final product antenna which is a passive patch antenna array of size 20 cm × 20 cm as proposed in [4]. The RX antenna used for testing is a standard rectangular horn antenna with a gain of TBD.
TX Power	$\leq$ -6	dBm	This is calculated from the EIRP regulations and the TX antenna gain. Higher powers can violate the ISM standard.
Range	$1.5 \leq R \leq 30$	m	The radar minimum and maximum ranges.
Range Resolution ΔR	Not required	NA	The function of this radar is to detect the targets with no requirement on range separation between them as the tagged moths will be aestivating in large groups.
Velocity	Not required	NA	The tagged moth is assumed to be stationary, no velocity measurements are required.

TX Pulse Duration	≤ 10	ns	For Pulsed waveforms the TX pulse duration should be less than the minimum range round-trip delay to be able to detect targets at the minimum range of 1.5 m.
PRI	≥ 200	ns	The pulse repetition interval should be more than the maximum range round-trip delay to be able to unambiguously detect targets at the radar maximum range of 30 m.
SNR	≥ 6	dB	To get good probability of detection P_D the signal to noise ratio after processing gains should be positive with a good margin.
f_{sweep}	50	MHz	For the FMCW radar the sweep frequency equals to the modulation bandwidth.
T_{sweep}	1	ms	For the FMCW radar the sweep time should be higher than 200 ns which is the round-trip time of the furthest target.

Table 5.1: System Specifications.

The radar system considered for this design is according to the block diagram in Figure 3.8. Detailed chain analysis and components selections are discussed in the rest of this chapter.

5.2   Radar Transmitter Design and Simulation

Figure 5.1 shows the radar transmitter schematic diagram. The aim for the transmitter design was to reduce the number of components and simplify the design to reduce the size and the power consumption of the overall system while maintaining minimum spurious and unwanted emissions.
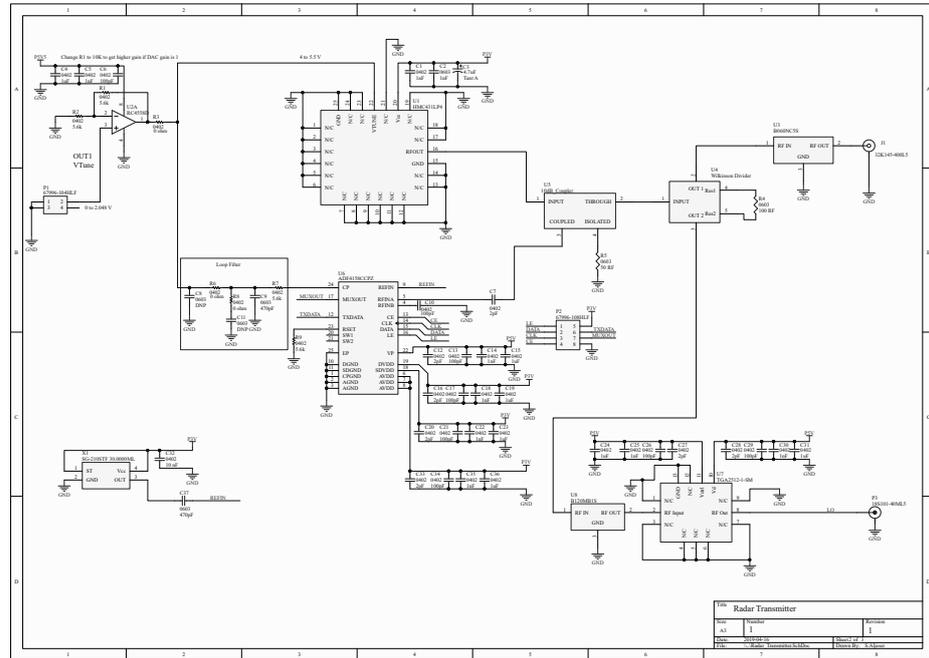
Figure 5.1: Radar Transmitter Schematic Diagram.

5.2.1   RF Source

The best way to achieve transmitter requirements is by using a clean low noise VCO component which can directly produce the required transmission frequency without using frequency multipliers or modulators. It is also required to produce double the frequency of the transmitted wave to be used as a local oscillator for the radar receiver. It is better to use exactly the same component to produce both signals to keep them tuned together and provide precise measurement of the beat frequency at the radar receiver. The Analog Devices HMC431LP4 was selected since it produces the required signal with an output power of 2 dBm, it covers the total required bandwidth with a considerable margin. It also produces the second harmonic signal of the generated signal with an acceptable level of -15 dBc compared to the fundamental signal. The component suppresses the DC power from the RF output port and have a simple pinout with ground pins shielding the RF pin for better grounding. It requires a total supply current less than 30 mA at a DC voltage of 3 V. The Single Side Band SSB phase noise is very low, well below the requirement of out of band transmission for the ISM regulations.

The V_{TUNE} pin which is used to control the oscillator frequency output is internally filtered in the chip from high frequency interference.

VCOControl

The VCO can be directly controlled by a DAC to perform the transmission modulation, however most DACs use a full scale output of around 2 V_{pp}, hence it requires some voltage gain. An operational amplifier OP-AMP is used to shift the output of the DAC to the required control voltage for the VCO , which is according to the VCO datasheet in Appendix-C between 4 V and 5 V. The Texas Instrument RC4558 OP-AMP is used to amplify the V_{TUNE} voltage and supply it to the VCO . It is chosen because of the low power consumption, low noise output and the wide gain bandwidth capability which is required to cover the frequency sweeps within the sweep time. A simple non-inverting configuration is used as shown in the top-left corner of the schematic diagram in Figure 5.1. A 10 KΩ resistor is used for $R1$ the feedback resistor to give higher voltage gain according to the following equation:

$$A_v = 1 + \frac{R1}{R2} = 1 + \frac{10 \times 10^3}{5.6 \times 10^3} = 2.79 v/v \qquad (5.1)$$

Where

- A_v OP-AMP voltage gain.
- R1 is the feed back resistor.
- R2 is the inverting input resistor.

A MATLAB code is used to analyse the required tuning voltage steps, the code is attached in Appendix-A. The DAC component used for this system is part of a DAC/ADC module specific for the Raspberry Pi computer and will be covered in section (5.5).

Free-Running VCO vs. PLL

The design proposed so far assumes we are using a free-running VCO , which means the output RF signal is produced without checking its phase or frequency and assuming that the VCO is accurate enogh and will exactly produce the required frequency. From the datasheet of the VCO it is clear that the output frequency to tuning voltage response is non-linear which results in two big problems; the non-linearity of the output frequency sweeps and the inaccuracy of the output frequency at a given voltage. This causes the radar receiver to have changing baseband frequency and will effect the FFT processor by reducing the FFT resolution and affecting the range measurement accuracy of the radar system. To solve these problems, some sort of feed back between the generated output RF signal and the tuning voltage should be used. A common solution is to used a Phase Locked Loop (PLL) synthesizer. A PLL is a basic control system which uses feed-back from the output RF frequency from the VCO and compare it to a known clean reference oscillator and then controls the tuning voltage of the VCO accordingly, if the frequency or phase in this case is exactly the same, then the PLL is said to be locked and there will be no changes on the tuning voltage of the VCO . If there is a phase error between the two signals of more than a design threshold the PLL will detect this error and generates a voltage error to compensate for the

phase error and re-tune the VCO to get the exact required output voltage. This process is continuous through the operation of the PLL synthesizer to keep the output signal of the VCO locked and accurately produce the required frequency for transmission. A basic PLL block diagram is shown in 5.2 [3].
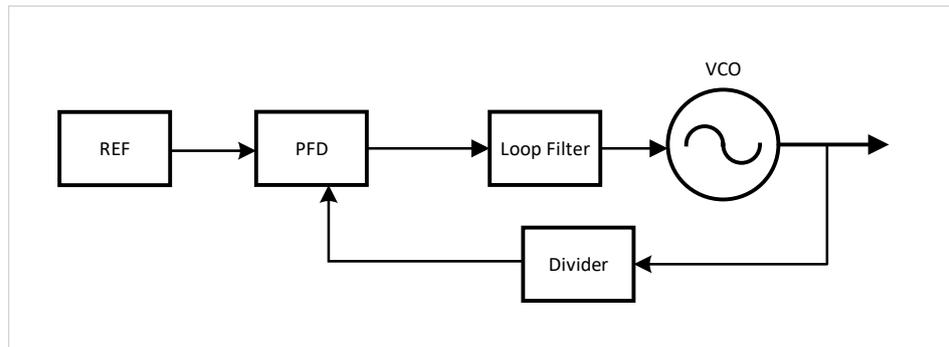

Figure 5.2: Basic Block Diagram of PLL Synthesizer.

There are four basic components of the PLL namely; Reference crystal (REF), Phase Frequency Detector (PFD), Loop Filter, and a frequency divider.

REF

The REF crystal is selected to be accurate and of very low phase noise, it is also required to be stable during the operation of the synthesizer. A common problem with the operation of crystals is the drift caused by ambient temperature and the aging effect of the crystal piezoelectric material. The aging effect is less of a problem since it occurs in a longer period often specified in years and can be selected very low down to several parts per million (ppm) of the oscillator output. The temperature effect can cause high errors in short duration, so a Temperature Compensated Crystal Oscillator TCXO is most often used to have more stable outputs.

Divider

Since the available crystal oscillators are usually a small cut from a piezoelectric material, they have fixed frequencies and they are usually not exceeding tens or at most hundreds of MHz, it is required to divide the frequency of RF output from the VCO down to a comparable level with the TCXO frequency, the frequency divider is used to do so. The divider can have fixed or tunable division ratios, depending on the divider control unit, the divider can be set to give large number of frequency steps to support the output frequency sweeps of the VCO while keeping the TCXO fixed.

PFD

The PFD is the main component of the PLL since it detects the frequency deviation of the output signal and provides the error correction signal to compensate for the deviation. It comprises phase detectors such as mixers or XOR logic gates to detect positive and negative phase errors and charge pump circuits to provide the positive and negative current outputs to compensate for the phase errors. It works by checking the differences in phase between the coupled and the reference signals since frequency drifts cause phase drifts. Then if a phase difference of less than $\pm 2\pi$ is detected either positive or negative the PFD generates a positive or negative output current by activating the charge pumps circuits at the output stage of the PFD for a time duration proportional to the amount of phase error. Once the phase error reaches zero, or a minimum threshold, the PFD enters a phase-locked mode and provides zero output current. The PFD is different than the simple phase detector PD by having three modes of operation instead of two; frequency detect, phase detect, and phase locked modes. When the phase difference is more than $\pm 2\pi$, the PFD switches to frequency detect mode and compensate for the frequency difference by generating a constant output current out of the charge pump circuits over time which results a continuously changing VCO tuning voltage, while the simple PD fails to detect frequency difference since it does not have a frequency detect mode.

Loop Filter

The loop filter is used to integrate the current output from the charge pump over duration to produce voltage error signal to be fed to the VCO. Loop filter can be passive or active, if the required voltage level for the VCO V_{TUNE} is higher than what the PLL can generate, then an active loop filter is required, otherwise a passive loop filter is sufficient.

PLL Design

Analog Devices ADF4158 is used as a PLL chip with built-in fractional divider to provide the required frequency steps for the FMCW frequency sweeps. The component datasheet is included in Appendix-C. The component is designed for FMCW radar functionality and it has specific settings for performing different FMCW waveforms. It covers RF frequency up to 6.1 GHz, which cover the frequency requirement for the radar system. It has an internal fractional-N divider with subhertz steps to provide the frequency steps required for FMCW sweeps. It has a simple 3-wire serial interface for setting the required waveform and parameters. Its performance is guaranteed for reference crystal source of frequency less than 32 MHz. It requires a voltage supply of 3 V and has a maximum load less than 32 mA. A 30 MHz SG-210STF TCXO crystal from EPSON Corp. has been chosen as a reference for the PLL synthesizer, it has very low output phase noise and has low frequency aging of 3 ppm/year. The component datasheet is included in Appendix-C for referincing. According to the FMCW waveform design, it is required to sweep a full range of frequency band of 50 MHz in 1 ms. This has to be done continuously with a large number of frequency steps. The ADF4158

provide its RF output according to the following equation:

$$RF_{OUT} = f_{PFD} \times \left(N + \left(\frac{FRAC}{2^{25}} \right) \right) \tag{5.2}$$

Where

- RF_{OUT} is the RF Output frequency of the VCO.

- f_{PFD} is the comparison frequency of the phase-frequency detector.

- N is the initial division of the internal 12-bit counter which range from (23 to 4095).

- FRAC is the 25-bit fractional division numerator ranging from (0 to 2^{25} -1).

The RF_{OUT} in our design range from 5.8 GHz to 5.85 GHz and the f_{PFD} is fixed at 30 MHz which is the frequency of the reference crystal. This give a requirement for the division ratio from 193.333 to 195 according to 5.2, This can be achieved by setting the N divider to 193 and changing the FRAC divider with each frequency step. The frequency resolution f_{RES} for each frequency step can be calculated as follows:

$$f_{RES} = \frac{f_{PFD}}{2^{25}} = \frac{30 \times 10^6}{2^{25}} = 0.894 Hz \tag{5.3}$$

The number of frequency steps depends on how fast the chip can sweep, since it is required to complete the entire sweep during 1 ms then frequency stepping should be performed as follows:

$$T_{step} = \frac{T_{sweep}}{N_{steps}} \tag{5.4}$$

Where

- T_{step} is the time required for each frequency hop.

- N_{steps} is the number of frequency hops.

The number of frequency hops also determines the frequency deviation for each hop. As an example if 200 frequency steps are required then,

$$f_{step} = \frac{f_{sweep}}{N_{steps}} = \frac{50 \times 10^6}{200} = 250 KHz$$
$$T_{step} = \frac{T_{sweep}}{N_{steps}} = \frac{1 \times 10^{-3}}{200} = 5\mu s \tag{5.5}$$

As the number of steps increase, the step frequency f_{step} decreases and as a result finer steps of RF_{OUT} hence finer range measurement is possible, to be able to detect the required range which corresponds to an f_{beat} range between $1KHz \leq f_{beat} \leq 20KHz$ it is required to have a frequency step of at least 1 KHz which correspond to a huge number of steps of 50000 and requires a step time T_{step} of less than 20 ns. It is not clear from the PLL datasheet if it can

perform this number of steps in a fast time, however since there will be a loop filter after the PLL charge pump to drive the control voltage to the VCO, then it will average the output voltage over time to give finer steps. So even if the PLL cannot achieve the requirement for finer steps, the loop filter will do. The passive loop filter is designed from lumped components since the PLL chip can produce the required tuning voltage from the supplied 5 V DC at the VP pin. A room for higher order filter has been considered but a 1st order lumped element low-pass filter has been designed and optimized to the required cutoff frequency. Choosing lower frequency loop filter causes the loop to go out of locking from the high frequency noise, and choosing a higher frequency for the loop filter affects the frequency sweeps and can filter out the modulation frequency. A 60 KHz low-pass loop filter was designed according to the simulations performed in ADIsimPLL tool from Analog devices. Figure 5.3 shows the synthesizer simulation results. A MATLAB model for the PLL calculations along with VCO DAC control voltages is included in Appendix-A.
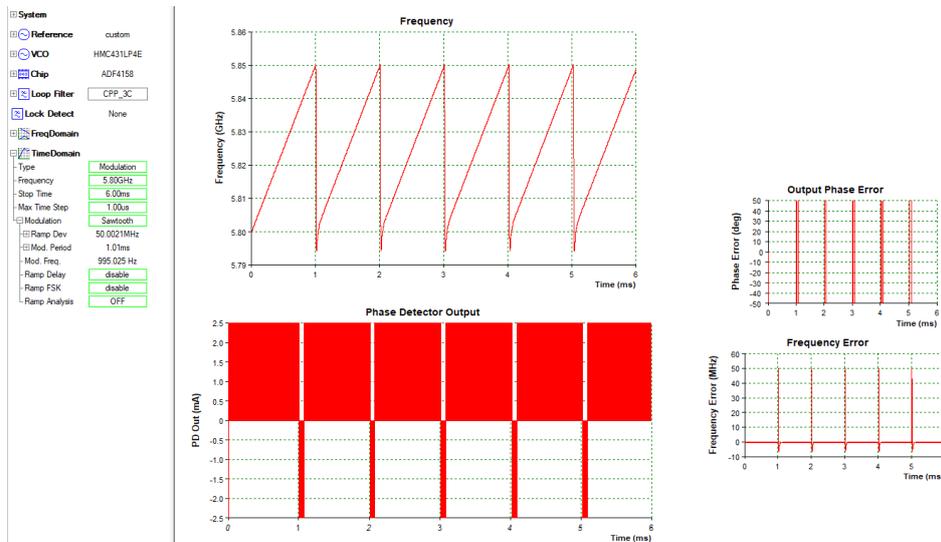

Figure 5.3: Simulation of ADF4158 PLL and HMC431LP4 VCO Synthesizer.

5.2.2   Coupling and Division

To provide the PLL with a copy of the transmitted signal a coupler can be used
with enough coupling to feed the PLL with the required signal power and enough
isolation to prevent interference on the transmitted signal. A Micro-Strip (MS)
printed circuit directional coupler is used with a coupling of 12 dB and a directivity
of 20 dB to provide the required isolation. The coupler is designed and simulated
in CST CAD tool, detailed description and results are provided in section (5.7).
It is required to provide a copy of the transmitted signal to the receiver to act as
a LO for the frequency down-conversion. This function is done using a MS 2-Way
Wilkinson Power Divider printed circuit. The Wilkinson divider splits the TX
signal into two equally powered signals with minimum ohmic losses and around
3 dB division loss for the transmitter and the receiver LO. It also provides good
isolation between the two signal paths of around 30 dB to prevent reflections from
the RX path to the TX path and keep the transmitter as clean and isolated as
possible. A divider is chosen instead of the coupler to provide enough RF signal
power to drive the LO. The dividerr is designed and simulated in CST CAD tool,
detailed description and results are provided in section (5.7).

5.2.3   Filtering and Amplification

The ISM band requirements in [1] specifies the out of band transmission to be
-40 dBc which requires a high suppression band-pass filter to suppress the out of
band emissions of the radar transmitter. It is difficult to achieve a similar filter
with printed circuit technology to provide the required filtering with a high quality
factor. A special cavity RF band-pass filter is used to perform this function. The
DIELECTRIC LABS B060NC5S band-pass filter has a minimum of 65 dB out of
band rejection and a maximum insertion loss of 3 dB. It has a 60 dB bandwidth
of 3 GHz at a center frequency of 6 GHz, it is ideal for our application to suppress
the harmonics generated by the VCO way below the required -40 dBc. The filter
datasheet is included in Appendix-C. The level of the TX signal after filtering is
still acceptable and the transmitter does not require a TX amplifier to drive the
TX antenna.
The LO signal is taken as the second harmonic of the VCO output to be used
at the receiver to generate the beat frequency of the FMCW. It is important to
filter out the fundamental signal frequency since it can cause high order inter-
modulation effects which can be close to f_{beat} and produces false alarms. Another
BPF is used to pass the 2nd harmonic and suppress the fundamental signal. The
DIELECTRIC LABS B120MB1S band-pass filter has a minimum of 55 dB out of
band rejection and a maximum insertion loss of 3 dB. It has a 50 dB bandwidth of
2.5 GHz at a center frequency of 12 GHz, it is ideal for our application to suppress
the other harmonics generated by the VCO way below the required -40 dBc and
pass the 2nd harmonic. The filter datasheet is included in Appendix-C. The level
of the coupled LO signal to the receiver path is small and will not be sufficient to
drive the down-converter. A linear amplifier is required to amplify the signal to the
required level. As will be mentioned later in this chapter, the required gain of this
amplifier is at least 20 dB in order to achieve a power level more than 0 dBm at
the down-converter LO pin. TriQuint TGA2512-SM low-noise amplifier has been

chosen to amplify the signal with minimum additional noise and prepare it for the down-converter. It has a gain of 21 dB and can produce a linear output signal up to 6 dBm. It requires 90 mA of supply current at 5 V DC voltage. The amplifier datasheet is included in Appendix-C. A wide range of decoupling capacitors have been selected for the LNA power and control voltage pins starting from 2 pF up to 1 μF, more about capacitor selection will be discussed in section (5.8).

This concludes the transmitter components used for the radar system. Some simulations have been performed in MATLAB, CST CAD tool and other manufacturers specific CAD tools to analyze the performance of the selected components and study the compliant to the system specifications. The PLL simulation and analysis has already been covered earlier, the directional coupler and the Wilkinson divider has been designed in CST CAD tool and the results are included in section (5.7) along with PCB tracks simulations.

5.3   Radar Receiver Design and Simulation

Figure 5.4 shows the radar receiver schematic diagram. It is required to design the radar receiver at twice the frequency of the radar transmitter. The expected range of received frequencies are from 11.6 GHz to 11.7 GHz.
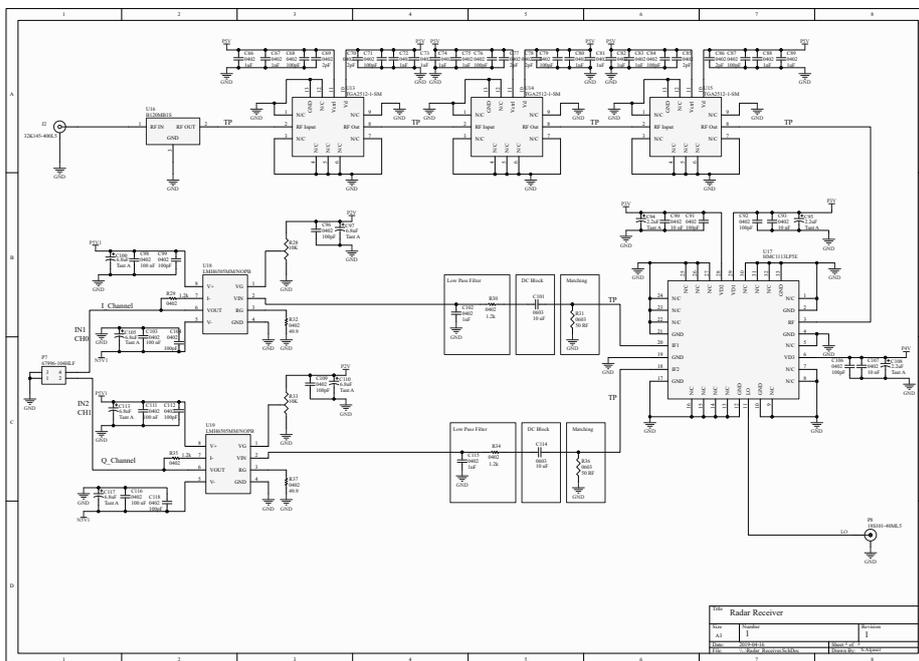

Figure 5.4: Radar Receiver Schematic Diagram.

5.3.1   RX Filtering

To prevent the radar receiver from receiving at the TX frequency, a high rejection BPF is used. The same filter used for LO filtering has been used for RX signal filtering since it provides the required level of performance.

5.3.2   RX Amplification

High amplification gain is required at the radar receiver since the received signal is very weak due to path losses and very weak signal reflections from the tagged moths. a minimum of 60 dB of amplification is required according to link budget analysis made in chapter 3. A detailed link budget analysis will be covered following in this chapter. Three LNAs has been used in cascade to provide the required RX gain and maintain minimum noise level. The same TGA2512 LNA used for LO amplification is used for RX amplification since it has enough gain of 21 dB and has a maximum noise figure of 2.5 dB. This give a total cascade gain of almost 60 dB and a total cascade NF of 4.5 dB for the three amplifiers including the RX BPF. Careful decoupling capacitors has been chosen to decouple the DC voltage supplies to the LNAs and prevent spikes on the voltage line caused by current demands which can cause inter-modulation effects at the output of the LNAs, more about capacitor choices will be discussed in section (5.8). Also careful considerations about the placement, routing and grounding of the cascaded amplifiers have been performed to prevent ground loops and coupling between different inputs and outputs more of this is included in section (5.7).

5.3.3   RX Down-Conversion

An IQ down-converter is used for generating the RX beat frequency from the RF received signal and the LO coupled from the currently transmitted RF signal. The output of the down-converter is a complex signal with two components; in the I (in-phase) and Q (quadrature-phase) domains. This is important to perform the complex FFT process at the radar processor and measure the range of the reflected signal. The down-converted signal will be directly in the base-band frequency, however other inter-modulation components will be generated by the mixer. So it is important to filter the output of the mixer with a low-pass filter at sufficient cutoff frequency above the maximum expected f_{beat}. Analog Devices HMC1113LP5 downconverter has been used. It is an active IQ mixer operating from 10 GHz to 16 GHz and produce two IF outputs from DC up to 3.5 GHz. It requires a total of 160 mA of supply current at 3 V and 4 V DC voltages to drive the two internal amplifiers for the RF and LO signals. It has 12 dB of conversion gain and only less than 2 dB of NF. It is also made for radar applications. The component datasheet is included in Appendix-C. A DC block is required after the down-conversion to protect the receiver from high DC voltages which can harm or saturate the receiver ADC. A 10 μF capacitor has been used in series to block the DC voltages and pass the minimum f_{beat} of 1KHz since it has an impedance of 16Ω at 1KHz and 0.8Ω at 20KHz. For the RX filtering a lumped elements LPF is designed to cover the maximum f_{beat} of 20 KHz. A simple RC LPF has been

designed to have minimum attenuation at the required beat frequencies. $1.2K\Omega$ resistor and 1nF capacitor have been used with a cutoff frequency of 132 KHz.

5.3.4 Automatic Gain Control AGC

Long range and short range targets have different signal powers since they are subjected to different path losses according to the Friis transmission formula. If this power difference is high then it can cause problems to the radar receiver especially if it is higher than the receiver dynamic range. Either the long range target signal is too weak to be detected or the short range target signal is too high which can saturate the receiver. In our design the power difference is almost 50 dB. To solve this issue, different techniques can be used, one common technique is to use adaptive amplification such as AGC at the receiver. An AGC works by amplifying the received signal to the maximum amplification level and checking the output voltage level. If the voltage level exceeds a certain threshold, the AGC reduces the gain until it reaches an acceptable level. An AGC usually has a large range of gain adjustment. For our design we have selected an AGC with 80 dB of voltage gain range to adapt to the changes in RX voltage. A MATLAB code for analysing the RX voltages and the required AGC adjustment has been made and included in Appendix-A. The component selected for AGC is the Texas Instruments LMH6505 which has a wide unity gain bandwidth of 100 MHz can drive heavy load ADC up to 60 mA. The chip has an adjustable VG pin to detect the output voltage and change the gain accordingly. The total amplifier gain is calculated from the gain-range resistor R_G and the feedback resistor R_F as follows:

$$A_{VMAX} = \frac{R_F}{R_G} \cdot K = \frac{1.2 \times 10^3}{50} \cdot 0.94 = 22.56 v/v \qquad (5.6)$$

Where K is a gain multiplier of the LMH6505 device. This sets the maximum voltage gain of the AGC to $22.56v/v$ or 27 dB, however this gain can be controlled using the VG pin by supplying a voltage between 0 V to 2 V, where 2 V gives the maximum gain and 0 V reduces the gain by almost 80 dB. In our design we chose to control this manually using a potentiometer, it can be changed easily in the future and a connection to an external DAC can be made from the control pin to be able to digitally control it. This choice has been made to simplify the control system as much as possinle and reduce the required number of components.

This concludes the receiver and transmitter designs, the only components not covered so far are the ADCs and the DAC, they are part of the radar processor design and will be included in section (5.5).

5.4 Detailed Link Budget Analysis

Now that all the main components for the radar receiver and the radar transmitter are selected a detailed description of the link budget analysis is performed, the analysis has been made in MATLAB and the code is included in Appendix-A. A detailed block diagram with notations of Signal and noise powers is shown in Figure 5.5
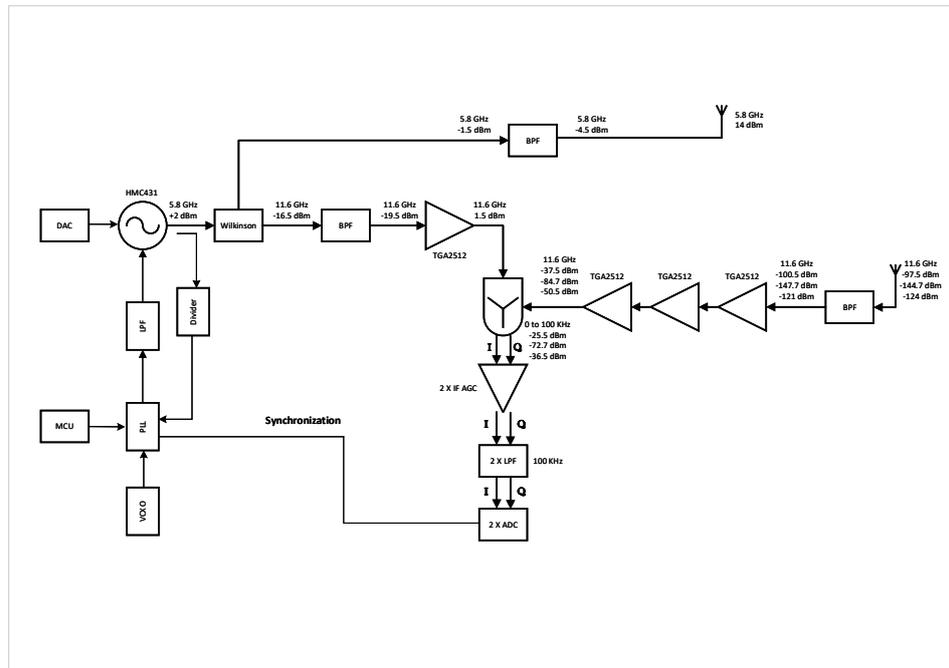
Figure 5.5: Radar System Budget Analysis.

5.5 Radar Signal Processor

The radar processor is a major part of the radar system it is responsible for generating the TX waveform, PLL control, controlling the ADC/DAC components, AGC gain setting, performing the processing functionality of the radar including filtering, averaging, FFT processing and time integration. It is also required to be user friendly. The best way for optimizing the radar performance is to design a specific digital processor optimized for the required functionality and for minimum power consumption, components size and cost. This will be true if the system is aimed for production, however in our case we are designing a proof of concept. For this a Raspberry Pi 3B computer has been chosen to serve as a processor/controller for this radar system, because of its small size, light weight, low power consumption, high capability and wide range of applications. The Raspberry Pi can be programmed in Python or in C. It has a quad core ARM processor clocked at a maximum frequency of 1.2 GHz and a RAM of 1 GB. A transmitter script has been coded and tested in Python to generate the DAC signal for VCO sweeping in the transmitter. The script is installed and tested in the Raspberry Pi processor. A daughter ADC/DAC board from ABELECTRONICS designed specifically for the Raspberry Pi has been procured, it has limited capabilities but it gives acceptable performance for the functionality of this radar. It has 12-bit dual channel ADC and 12-bit Dual channel DAC. The ADC has a maximum sampling rate of 100 Ksps which can sample the received maximum beat frequency of 20 KHz with a good margin . The DAC supports a clock of 20 MHz at a full-scale output of

2.048 V which can generate the required VCO tuning voltage within 1 ms however the voltage level should be increased by using the designed OP-AMP with a gain of 2.79v/v to provide the required V_{Tune}.

5.6   DC Power Supply Design

Figure 5.6 shows the radar DC power supply schematic diagram. It is required to generate four different voltage levels to power all the components. The power source can be from the USB cable connected to the Raspberry Pi or from an external battery with input voltage levels from 2 V to 16 V.

Voltage	Component	Current	Power	Total Power
5 V	4×TGA2512-SM LNAs	90 mA	90 mA×5 V = 0.45 W	4×0.45 = 1.8 W
5 V	Raspberry Pi	400 mA	400 mA ×5 V = 2 W	2 W
4 V	HMC1113 down-converter	100 mA	100 mA ×4 V = 0.4 W	0.4 W
3 V	HMC1113 down-converter	60 mA	60 mA ×3 V = 0.18 W	0.18 W
3 V	HMC431 VCO	27 mA	27 mA ×3 V = 0.081 W	0.081 W
3 V	ADF4158 PLL	32 mA	32 mA ×3 V = 0.096 W	0.096 W

Table 5.2: DC Voltage Distribution.

Table 5.2 shows the major supply requirements for the radar components. It shows that the total required DC power is below 5 Wh. However, this depends on the efficiency of the DC regulators. All regulators have been simulated in the TI WEBENCH. The simulation results are included in Appendix-C.

5.7   Detailed RF Components Design and Simulation

Some components have been designed in CST to check their performance, the 2-Way Wilkinson power divider and the 10-dB directional coupler has been designed and simulated. Track widths and lengths have been optimized in CST to get the required performance, some simulation results have been included. The PCB designed is a simple 4-layers symmetric RF PCB using the Rogers RO4350B dielectric material which is suitable for most RF circuit applications. The total PCB thickness is 1.5 mm but the continuous RF ground is the closest layer to the top layer giving a dielectric thickness of 0.508 mm. The RO4350B material has a low tangential loss of 0.0037 and a dielectric constant of 3.38 at X-BAND. PCB layer stack design in included in Appendix-B along with the manufacturing drawings.
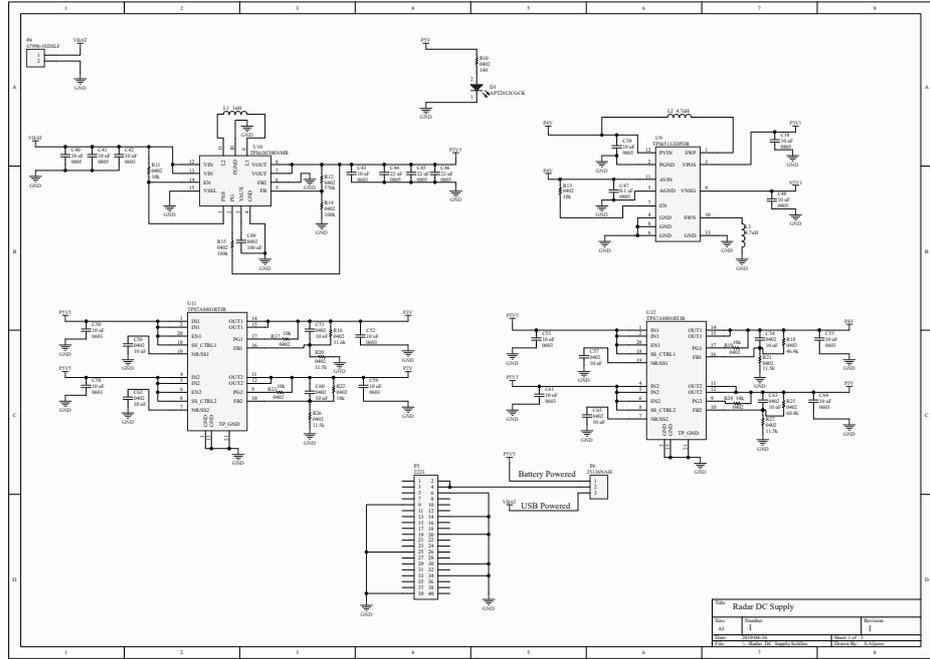
**Figure 5.6:** Radar DC Power Supply Schematic Diagram.

5.7.1 Wilkinson Power Divider

The divider is used to split the RF signal generated by the VCO into two paths; the TX path and the LO path for RX down-conversion. It should operate equally in both fundamental frequency 5.8 GHz and at the 2nd harmonic 11.6 GHz. The Wilkinson is designed with $\lambda/4$ branches to transfer the input impedance to the output impedance, since there is two output branches with 50Ω impedance, the impedance transformer should translate the input 50Ω impedance to a total output impedance of 100Ω. The transformer branches should be of 70.7Ω impedance and a length of $\lambda/4$ of the lowest frequency. This is calculated as follows:

$$Z_T = \sqrt{Z_{source} \cdot Z_{load}} = \sqrt{50 \times 100} = 70.7\Omega \tag{5.7}$$

The electrical length is calculated using a Microstrip line calculater and the required $\lambda/4$ length is around 8 mm. After doing the design on paper, it has been built in CST CAD as shown in Figure 5.8. The final component after optimization as shown in the figure has a square shape of around 8×8 mm.

The optimization parameters were, the S-parameters for transmission, reflection and coupling of the three divider ports. The goal was to reduce the ohmic losses below 1 dB of the divider, to have good reflection coefficient below -10 dB and to have good isolation between branches of better than 15 dB. A 100Ω wide-band surface mount resistor is used between the output branches to have a better output isolation. The results shown in Figure 5.7 are acceptable for the requirements of the divider, the transmission losses on each branch is around 3.5
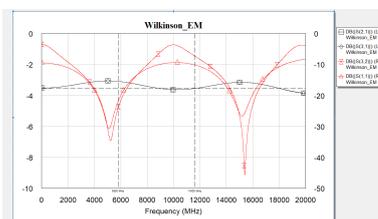
Figure 5.7: S-Parameters Simulation Results for The Wilkinson Divider.
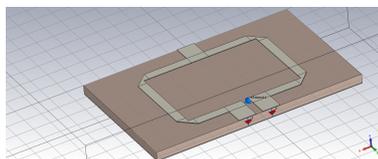
Figure 5.8: 2-Way Wilkinson Power Divider.

dB for both frequency bands, the reflection coefficient is below -20 dB for the TX frequency and around -10 dB for the LO frequency, the isolation between branches is below -20 dB for the TX frequency and around -10 dB for the LO frequency.

5.7.2 Directional Coupler

The directional coupler is used to feed the VCO output signal to the PLL circuit, it has to do this without disturbing the TX signal. A directional coupler is basically a $\lambda/4$ Microstrip line which is placed very close to the output line of the VCO. It uses the coupling between the Microstrip lines to generate a coupled version of the VCO output it also uses a 50Ω termination resistor at one of the coupled lines ends to give proper matching. The coupled signal direction will be opposite to main signal direction by basic EM theory. The component is designed numerically and built in CST CAD and then optimized for less insertion loss on the main path, higher coupling to get the required -10 dBm power level for the PLL circuit from the output of the VCO which is 2 dBm. It is optimized for better isolation and better reflection coefficients for both lines. The isolation is required to prevent opposite coupling from the PLL to the VCO , this is done by using a 50Ω wide-band surface mount resistor at the isolated port. Figure 5.10 shows the directional coupler in CST CAD tool with shielding Vias to prevent surface propagation The total component size is around 9×5 mm. Figure 5.9 shows the simulation results of the coupler with an insertion loss on TX path of less than 0.5 dB, a coupling to the PLL path of around 12 dB, an isolation of 25 dB and reflection coefficients of less than -10 dB.
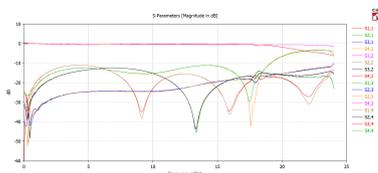

Figure 5.9: S-Parameters Simulation Results for The Directional Coupler.
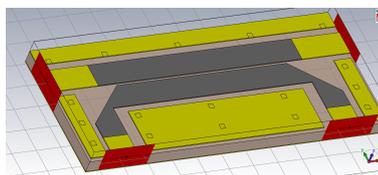

Figure 5.10: 10 dB Directional Coupler.

5.8   Components Selection

All the major components has been selected to give lowest possible power consumption, small size, light weight and achieve the required functionality of the radar system. One major issue with this application is that it will be installed in a flying drone which requires immunity to shocks and vibrations. Vibration causes interference to the RF signal since movement can create changes in voltages especially for solid structures such as ceramic components, this happens mainly in the ceramic capacitors for DC lines decoupling. This problem is often referred to as Microphonics which is sound emissions from ceramic components, it happens if the noise in capacitors is within the hearing sound frequency band then buzzing sound can be heard from noisy capacitors. To solve this issue special type of capacitors has been selected which has a raised bed called CoLF which absorbs the vibrations on the capacitors [8]. Another special components are the decoupling capacitor ranges, since components are susceptible to more noise because of the vibration of the drone wings, careful selection of decoupling capacitors has been considered especially for the VCO and the LNAs since they require clean supplies. A range from 2 pF up to 1μF capacitors has been selected to supply high current demands and reduce high and low frequency voltage noise on the power supply lines.

Manufacturing and Assembly

The initial plan was to perform PCB manufacturing in the university manufacturing LAB but since the LAB has not been tested before for multi-layer designs it was agreed to procure the manufacturing from outside. Corga, a PCB manufacturing facility near Gothenberg has been selected to manufacture the PCBs The cost for manufacturing five PCBs was the same as manufacturing one, they cost around 8000 Kroners. The design uses 4-layers Rogers4350B substrate with 0.508 mm thickness and a total PCB thickness of around 1.5 mm. It only uses top to bottom Via holes with sizes between 0.2 mm for thermal Vias under the surface mount components and 0.5 mm for the ground connection Vias. The manufacturing data-pack supplied to the PCB manufacurer is inculded in Appendix-B, it includes PCB layout for all four layers, Via holes positions, and PCB layer stack. Figures 6.1 and 6.2 show pictures of the manufactured PCBs.
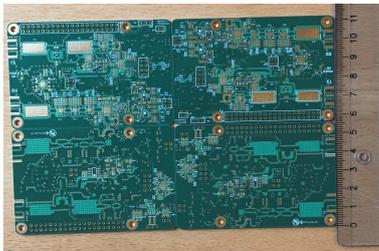

Figure 6.1: Harmonic Radar PCB Boards.
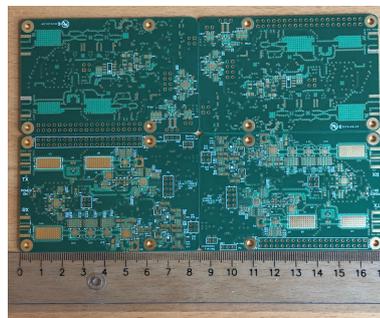
Figure 6.2: Harmonic Radar PCB Boards.

The PCB assembly is done in the university using the soldering facilities and by doing manual pick and place. Most of the components have been soldered in the Reflow oven and the solder paste was placed with the help of a flexible stencil made by one of the university engineers using a flexible film material as shown in Figure 6.3. The large connectors and jacks have been soldered by hand using the soldering station and the Microscope when required. Figures 6.4 and 6.5 show the Harmonic radar system after assembly of all components.
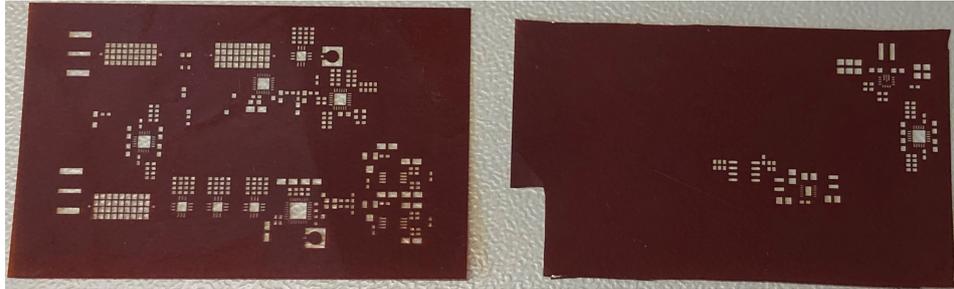
Figure 6.3: Top and Bottom Layers Stencils Using Flexible Film.

Figure 6.4: Harmonic Radar Af-
ter Assembly.

Figure 6.5: Harmonic Radar Af-
ter Assembly.

After the components assembly the radar is integrated with the Raspberry Pi processor as shown in Figure 6.6 and is ready for the testing phase.

Figure 6.6: Harmonic Radar Integration.

Testing and Verification

Three types of testing have been performed to verify the performance of the radar against system requirements, and also against simulations and analysis.

7.1 Electrical Continuity Testing ECT

The ECT is performed on the PCB before components assembly to make sure all tracks and Vias are connected and routed as required. This is done by using a Ohmmeter and checking the resistance between tracks, pads and Vias and make sure that there are no short circuits or disconnections. After testing all the five PCBs we found that the PCBs had no disconnections and no faulty short circuits and the Vias and tracks are routed as expected.

7.2 DC Power Supply Testing

The aim of this test is to check the supply voltages generated and compare them with the designed voltages, also to check the full power dissipation of the radar. After the assembly process of all components, the radar is integrated with the Raspberry Pi processor and the TX script is installed and tested at different supply voltages, The PCB was operating from around 3 V up to around 10 V, it has not been tested with higher voltages, however it is designed to work up to 16 V. The full load current for the radar system at 5 V supply voltage was around 1 A. This gives a total power consumption of 5 Wh. A 5 V input voltage has been supplied to the Buck/Boost converter regulator at the battery pin of the harmonic radar then all the voltages generated by the regulators are tested and verified to be as expected. Also the full load current has been recorded to be around 1 A. This gives a total power consumption of around 5 Wh as expected, this is shown in Figure 7.1

Figure 7.1: DC Supply Full Load Testing.

7.3 Functional Testing

After integrating the harmonic radar with the Raspberry Pi and the ADC/DAC PCB the Python TX script is tested and the output of the TX SMA port is recorded. The test setup used for the functional testing includes:

- A DC Power Supply capable of generating 5 V and 1.1 A.

- A Spectrum Analyser capable of testing frequencies up to 12 GHz.

- A Multi-meter to measure the voltages and connections of all components.

- An Oscilloscope to measure the DAC V_{Tune} sweeps.

The TX output is shown in Figure 7.3. It is shown the the output at the 2nd harmonic frequency is higher than expected, it seems that the TX filter is not working properly. The reasons could be fringing fields over the filter or bad Via

Figure 7.2: TX Output Test Setup.
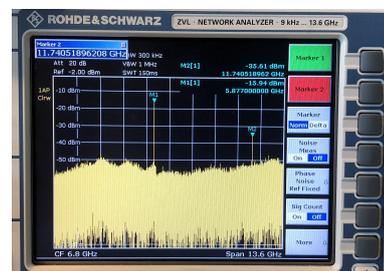
Figure 7.3: Spectral Measurements of TX Output Port.

shields around the RF routs. To make sure, some Aluminum conductive tape has
been placed on top of the filter and the RF path to the TX port and the output
of the TX port is measured again to check if it is improved. Figures 7.4 and 7.5
show the modification an the measurements results after the modifications. It is
shown that the 2nd harmonic frequency is suppressed as expected, this proves that
the problem was from the fringing fields.
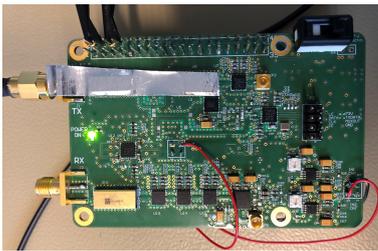
Figure 7.4: TX Output Test
Setup With Modifications.
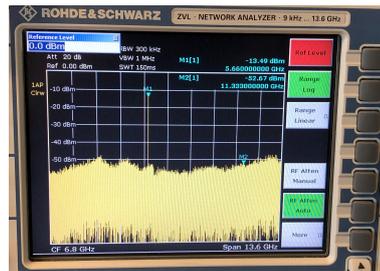
Figure 7.5: Spectral Measure-
ments of TX Output Port Af-
ter Modifications.

The RX path is tested by injecting the TX signal to the RX SMA port; loop-
back test. Then measuring the RX output after the LNAs using a coaxial probe.
The RX output is shown in Figure 7.7. It is shown that the output is lower than
expected, the LNAs are not working properly.
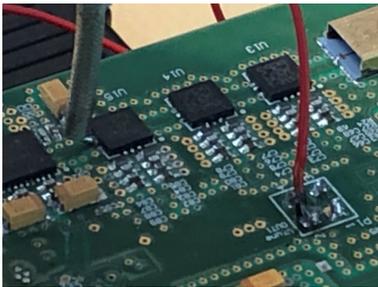
Figure 7.6: RX Output Test
Setup.
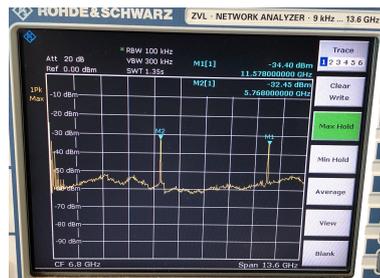
Figure 7.7: Spectral Measure-
ments of RX Output Port.

This can be an effect of fringing fields as well. A similar modification is made
using the Aluminum tape over the LNAs to check if the results are improved. The
measurements have improved as expected, the results are shown in Figure 7.9.
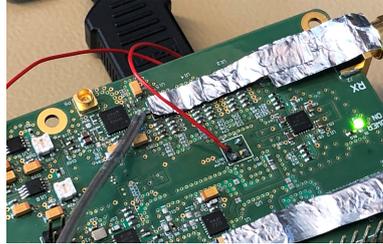
Figure 7.8: RX Output Test Setup With Modifications.
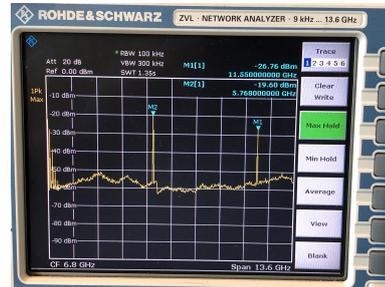
Figure 7.9: Spectral Measurements of RX Output Port After Modifications.

7.4 Thermal Testing

After performing all functional tests the system was operational for at least two hours continuously and the PCB was too worm especially around the LNAs and the RX path. A thermal camera has been used to measure the components and PCB junction temperatures at different places of the PCB. It has been found that the LNAs have the highest temperature increase to about 86°. This is due to the limited space around the LNAs which results on limited heat dissipation from top layer to the ground layer. Figure 7.11 shows a thermal image of the PCB showing the temperature rise.
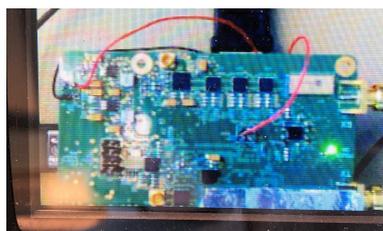

Figure 7.10: Thermal Testing Setup.

Figure 7.11: Thermal Image of the RX LNAs

A modification has been made to reduce the temperature rise by using a heat sink over the LNAs. The temperature after placing the heat sink dropped significantly as shown in Figure 7.13, with proper application of thermal paste the temperature can be reduced further.
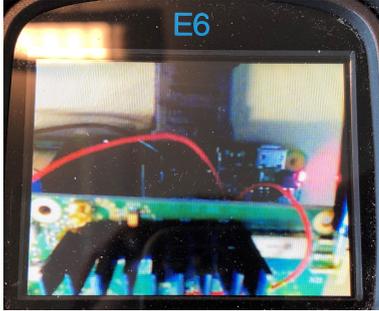
**Figure 7.12:** Thermal Testing Setup With Modifications.
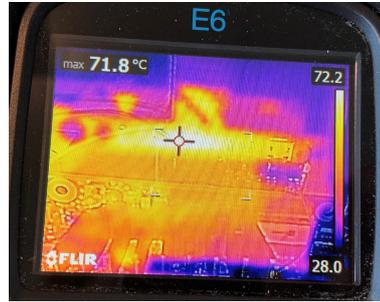
Figure 7.13: Thermal Image of the RX LNAs After Modifications.

As a summery of the testing stage, the test results show that:

- PCB manufacturing was successful and performed according to the design requirements with no short circuits or disconnections.

- Components assembly was successful since all pads were tested and found to be connected as required.

- DC power supplies are functioning as required generating all required voltages (5.5 V, ± 5 V, 4 V, 3 V, and 2 V) from input voltage source in the range between 2 V to 16 V.

- The total power consumption of the radar is within the expected figure around 5 Wh with all components active and the Raspberry Pi processor at full performance.

- The functional testing of the radar transmitter shows that the transmitter operates as expected but with lower TX power. The expected TX power was -5 dBm, while the measurements show a maximum TX power of -14 dBm with almost 9 dB of TX losses. The measurements show as well that the TX harmonics are suppressed as expected after the modifications performed.

- The functional testing of the radar receiver shows that the receiver does not provide enough amplification and out-of-band suppression. The modifications performed have improved the receiver performance, but still the measurements are below the expected results. The loop-back test shows that the total measured RX gain is around 30 dB instead of 63 dB. And the out-of-band suppression is around 10 dB instead of the expected 40 dB out of the RX BPF. This can be due to surface propagation or improper soldering around the RX filter. To investigate this issue, more testing and investigations are required.

- The radar processor testing shows that the DAC is capable of generating the required frequency sweeps within the required sweep duration of 1 ms, however when the Raspberry Pi starts fetching other processes, the sweep duration increases to around 7 ms. This requires proper settings for the

Raspberry Pi priorities to give higher priority for the radar TX sweeps tasks and have a stable TX performance.

- The ADC testing was not performed since the test setup was not complete. Measurements of the ADC data rate, and the FFT processes timing and integration gain has to be performed to validate the functionality of the radar receiver. This can be performed when the LO feeding cable is available.

Conclusion and Future Work

Developing a small harmonic radar for UAVs is a challenging task. It requires careful considerations of the size, weight, and power consumption of the whole system. Using the radar to detect small insects makes the design even more challenging due to the small reflections from the insects which puts more stress on the radar receiver requirements.

In the system design, different configurations have been studied then a candidate design has been selected to minimize number of components, system size, weight and power consumption. Initial design expectations using the link budget analysis indicated low SNR levels at the required radar operation ranges, this has been solved with a proper design of the radar waveform using a linear chirp FMCW radar waveform and an FFT processor at the radar receiver to improve the received SNR. As an attempt to simplify the radar transmitter design a simple DAC controlled VCO was implemented and tested, however to reduce the risk of high frequency variations at the radar RX an optional fractional-N PLL circuit was included. To reduce the risk of manufacturing defects, the manufacturing was procured from an external supplier. However the components assembly were performed in the university LABs.

The testing and measurements performed show that the radar is operational with some limitations in the receiver performance, however the system was declared as partially-successful and will comply to the system requirements.

The developed harmonic radar successfully serves as a proof of concept for the desired system, it is useful for testing different algorithms for insect detection and can be installed in a flying drone to perform field tests and provide the required functionality, however there could be some limitations in the maximum range of operation due to the receiver and processor limitations. It is important however, to spend more effort on improving the radar processor by procuring or building a dedicated processor optimized for the key functions of the radar system such as FFT implementations. It is also important to invest on a better ADC/ DAC components as they were the limiting factor of the radar performance. To reduce the cost it is advisable to look for less expensive RF filters or invest in developing them as they were the most expensive components.

Bibliography

[1] ETSI. Draft etsi en 302 502 v2.0.8 harmonised european standard, 2016. https://www.etsi.org/deliver/etsi_en/302500_302599/302502/02.00.08_20/en_302502v020008a.pdf.

[2] P. Fuks. *Harmonic Radar, a Modern Method for Location of Avalanche Victims*. TRITA / TET. Division of Electromagnet. Theory, the Royal Inst. of Technology, 1981.

[3] Floyd M Gardner. *Phaselock techniques*. John Wiley & Sons, 2005.

[4] Ze Fu Hamza Bin Faheem. Compact lightweight antenna designs for harmonic radar application, 2018. https://www.eit.lth.se/sprapport.php?uid=1139.

[5] Stanley Heinze and Eric Warrant. Bogong moths. *Current Biology*, 26(7):R263–R265, 2016.

[6] Miao-Lin Hsu, Shiang-Jie Jan, Zuo-Min Tsai, Huei Wang, Fan-Ren Chang, Pei-Hung Jau, Kun-You Lin, and En-Cheng Yang. Portable 9.4/18.8 ghz harmonic radar system using pulse pseudorandom code principle. In *2015 European Microwave Conference (EuMC)*, pages 885–888. IEEE, 2015.

[7] Jaewon Kim, Minhyung Jung, Hong Geun Kim, and Doo-Hyung Lee. Potential of harmonic radar system for use on five economically important insects: Radar tag attachment on insects and its impact on flight capacity. *Journal of Asia-Pacific Entomology*, 19(2):371–375, 2016.

[8] Mark Laps, Roy Grace, Bill Sloka, J Prymak, Xilin Xu, Pascal Pinceloup, Abhijit Gurav, Michael Randall, Philip Lessner, and Aziz Tajuddin. Capacitors for reduced microphonics and sound emission. *Assemblies Materials Association*, 04 2007.

[9] Göran Lindell. Introduction to digital communications. *Lund, Sweden: Ekop*, 2006.

[10] DANIEL MASCANZONI and HENRIK WALLIN. The harmonic radar: a new method of tracing insects in the field. *Ecological entomology*, 11(4):387–390, 1986.

[11] M. E. O'Neal, D. A. Landis, E. Rothwell, L. Kempel, and D. Reinhard. Tracking Insects with Harmonic Radar: a Case Study. *American Entomologist*, 50(4):212–218, 10 2004.

[12] Raoul Pettai. *Noise in receiving systems*. Wiley, 1984.

[13] Dimitris Psychoudakis, William Moulder, Chi-Chih Chen, Heping Zhu, and John L Volakis. A portable low-power harmonic radar system and conformal tag for insect tracking. *IEEE Antennas and Wireless Propagation Letters*, 7:444–447, 2008.

[14] Mark A Richards, Jim Scheer, William A Holm, and William L Melvin. *Principles of modern radar*. Citeseer, 2010.

[15] Zuo-Min Tsai, Pei-Hung Jau, Nai-Chung Kuo, Jui-Chi Kao, Kun-You Lin, Fan-Ren Chang, En-Cheng Yang, and Huei Wang. A high-range-accuracy and high-sensitivity harmonic radar using pulse pseudorandom code for bee searching. *IEEE Transactions on Microwave Theory and Techniques*, 61(1):666–675, 2012.

[16] Yan Wu and JPMG Linnartz. Detection performance improvement of fmcw radar using frequency shift. In *Proceedings of the 32nd WIC Symposium on Information Theory in the Benelux, Brussels, Belgium*, pages 1–8, 2011.

Software Scripts and MATLAB Codes

Tag Modeling MATLAB Code

```matlab
close all ; clear all; clc
%% Radar TX and Diode output Signals in Time Domain
Fc=5.8e9;                      % Frequency declaration
Fs=100e9; Ts=1/Fs;            % Sampling declaration
t=0:Ts:(1e-6)-Ts;             % time of TX sin wave
% n_t=1e-12*randn(size(t));   % Noise signal generated at RX
TX_Radar=sin(2*pi*Fc*t);
Diode_Output=zeros(1,length(TX_Radar));% Diode output is set to zero
%assuming signal is below diode threshold
for Time_Step=1:length(TX_Radar)
if TX_Radar(Time_Step)>=0    % Assuming Diode threshold voltage is 0.2.
    Diode_Output(Time_Step)= ...
        TX_Radar(Time_Step); % Diode output equals to radar TX when it
    %is above the diode threshold.
end
end
figure(1)      % Plots in Time Domain
subplot(2,1,1);
plot(t,TX_Radar)
title('Tx Wave 5.8GHz');
axis([0 500*Ts -1.5 1.5])
subplot(2,1,2);
plot(t,Diode_Output)
title('Diode Output');
axis([0 500*Ts -0.5 1.5])
%% Plots in Frequency Domain
L=2^nextpow2(length(TX_Radar));
f=Fs*(1:L/2)/L;
X_F1=fft(Diode_Output,L)/length(TX_Radar);
X_F=2*X_F1(2:L/2+1); % Diode output in Frequency Domain
X_FdB=20*log10(abs(X_F));   % dBW Diode output in Frequency Domain
figure(2) % Plot in Frequency domain Diode dBW
plot((f*1e-9),(X_FdB))
grid on
```

```matlab
grid minor
axis([0 f(end)*1e-9 -50 0])
ylabel('dB')
xlabel('Frequency [GHz]')
figure(3)    % Plot in Frequency domain Diode
plot((f*1e-9),abs(X_F))
grid on
grid minor
%% Diode Rx Voltage at 30 m Range from the Radar

Range=30; Freq_TX=5.8e9; Freq_RX=2*Freq_TX;
lambda_TX=3e8/Freq_TX; lambda_RX=3e8/Freq_RX;
Tag_Attenuation=20; Gain_ANT=22; EIRP=25e-3;
Path_Loss=10*log10((4*pi*Range/lambda_TX).^2);
Dipole_Gain=1.64; Dipole_Z=50;
Dipole_power=(10*log10(EIRP)) - Path_Loss + Dipole_Gain;     % dBW
Dipole_voltage=sqrt(10^(Dipole_power/10)*2*Dipole_Z);
```

Link Budget Analysis MATLAB Code

```matlab
close all; clear all; clc
Range=1:30; Sweep_BW=100e3;
Freq_TX=5.8e9+Sweep_BW; Freq_RX=2*Freq_TX;
lambda_TX=3e8/Freq_TX;lambda_RX=3e8/Freq_RX;
Freq_TX2=9.41e9; Freq_RX2=2*Freq_TX2;
lambda_TX2=3e8/Freq_TX2;lambda_RX2=3e8/Freq_RX2;
Ant_W=150e-3;Ant_L=150e-3;Ant_A=Ant_W*Ant_L; Ant_Eff_A = 0.65*Ant_A;
Gain_ANT_58=10*log10(4*pi*Ant_Eff_A/lambda_TX^2);
Gain_ANT_116=10*log10(4*pi*Ant_Eff_A/lambda_RX^2);
Gain_ANT_941=10*log10(4*pi*Ant_Eff_A/lambda_TX2^2);
Gain_ANT_1882=10*log10(4*pi*Ant_Eff_A/lambda_RX2^2);
Tag_Attenuation=20; Gain_ANT=22; EIRP=25;% ISM BAND 25 mW
Path_Loss1=[];Path_Loss2=[];PLE1=[];PLE2=[];Power_dBm=[]; Powerin_dBm=[];
figure(1)
for Range_Bin=1:length(Range)
    Path_Loss1(Range_Bin)=10*log10((4*pi*Range(Range_Bin)/lambda_TX).^2);
    Path_Loss2(Range_Bin)=10*log10((4*pi*Range(Range_Bin)/lambda_RX).^2);
    Path_Loss3(Range_Bin)=10*log10((4*pi*Range(Range_Bin)/lambda_TX2).^2);
    Path_Loss4(Range_Bin)=10*log10((4*pi*Range(Range_Bin)/lambda_RX2).^2);

    P_RX=(10*log10(EIRP))-Path_Loss1(Range_Bin)-Path_Loss2(Range_Bin)-...
    Tag_Attenuation+Gain_ANT_116; %dBm
    P_RX_1882=(10*log10(EIRP))+Gain_ANT_941-Gain_ANT_58-Path_Loss3...
    (Range_Bin)-Path_Loss4(Range_Bin)-Tag_Attenuation+Gain_ANT_1882; %dBm
    Amp1=amplifier('Gain',21,'NF',2,'OIP3',26);
    Amp2=amplifier('Gain',21,'NF',2,'OIP3',26);
    Amp3=amplifier('Gain',21,'NF',2,'OIP3',26);
    Amp4=amplifier('Gain',21,'NF',2,'OIP3',26);
    Amp5=amplifier('Gain',21,'NF',2,'OIP3',26);
    Amp6=amplifier('Gain',21,'NF',2,'OIP3',26);
```

```
    BPF_RX1 = rfelement('Gain',-3, 'NF',3);
    BPF_RX2 = rfelement('Gain',-3, 'NF',3);
    Mix_RX1=modulator('Name','Demodulator','Gain',12,'NF',2,'OIP3',13,...
        'LO',11.6e9,'ConverterType','Down');
    Mix_RX2=modulator('Name','Demodulator','Gain',12,'NF',2,'OIP3',13,...
        'LO',11.6e9,'ConverterType','Down');
    Budget=rfbudget([BPF_RX1 Amp1 Amp2 Amp3 Mix_RX1],Freq_RX,...
        P_RX,Sweep_BW);
    Budget_2=rfbudget([BPF_RX2 Amp4 Amp5 Amp6 Mix_RX2],...
        Freq_RX,P_RX_1882,Sweep_BW);
    SNR(Range_Bin)=Budget.SNR(end);
    SNR_2(Range_Bin)=Budget_2.SNR(end);
Powerin_dBm = [Powerin_dBm P_RX];
Power_dBm = [Power_dBm Budget.OutputPower(end)];
end
plot(Range,SNR,'r-o','linewidth',1.5);
title('SNR measured from different distances with 25mW EIRP');
ylabel('SNR [dB]');
xlabel('distance [m]');
hold on
plot(Range,SNR_2,'linewidth',1.5);
legend('5.8GHz TX, 11.6GHz RX', '9.41GHz TX, 18.82GHz RX');
grid on
grid minor
```

Barker Sequence Pulsed Waveform MATLAB Code

```
close all;clear all;clc
Barker_Sequence_13=[1, 1, 1, 1, 1, -1, -1, 1, 1, -1, 1, -1, 1];
N_chip=length(Barker_Sequence_13);
Auto_Corr=conv(Barker_Sequence_13,fliplr(Barker_Sequence_13)); % auto-correlation
figure
plot(-(N_chip-1):N_chip-1, abs(Auto_Corr./abs(max(Auto_Corr))));
xlabel('Normalized Time');title('Match Filter Response')
ylabel('Magnitude');
xlim([-14 14])
xticks(-14:2:14)
yticks(0:0.1:1)
grid on
grid minor
%%
Fc=100E6; N=100; Ts=1/Fc; Fs=N*Fc;
t=0:1/Fs:Ts-(1/Fs); G_T=sin(2*pi*Fc*t);
X_t=zeros(1,14998);
L1=length(G_T); G_f=fft(G_T,L1)/L1; f1=Fs*(0:L1/2-1)/L1; G_F=2*G_f(1:L1/2);
b=[];
for ii=1:N_chip
b=[b Barker_Sequence_13(ii) zeros(1,N-1)];
end
Y_t=conv(G_T,b); Y_t=Y_t(1:length(b));
```

```matlab
t_tx=0:1/Fs:((length(Y_t)/Fs)-1/Fs); x=0:0.01:13-0.01;
y=ones(1,length(x)); y(501:700)=-1*y(501:700); y(901:1000)=-1*y(901:1000);
y(1101:1200)=-1*y(1101:1200);
figure
subplot(2,1,1)
plot(x,y)
xlim([0 14]); xticks(0:14); ylim([-1.5 1.5]);
title('Baseband Barker Sequence')
xlabel('Normalized Time'); ylabel('Amplitude'); grid on; grid minor;
subplot(2,1,2)
plot(t_tx*1e9,Y_t)
ylim([-1.5 1.5]); xlim([0 140]); xticks(0:10:140);
title('RF Modulated Barker Sequence ')
xlabel('Time ns'); ylabel('Amplitude'); grid on; grid minor;
%% Pulsed Radar
R_min = 1.5; R_max = 30; c = 3e8;
tau = 2*R_min/c; PRI = 2*R_max/c ;tau_chip = tau/N_chip; DR = tau/PRI;
Fc=1/tau_chip; N=100; Ts=1/Fc; Fs=N*Fc;
t=0:1/Fs:Ts-(1/Fs); G_T=sin(2*pi*Fc*t);
L1=length(G_T); G_f=fft(G_T,L1)/L1; f1=Fs*(0:L1/2-1)/L1; G_F=2*G_f(1:L1/2);
%% Pulsed Vs CW Vs Modulated Pulsed
Temp=[];
for Time_Step=1:N_chip
Temp=[Temp Barker_Sequence_13(Time_Step) zeros(1,(length(G_T)-1))];
end
Pulse=[];
Conv_Period = [1 zeros(1,(length(G_T)-1))];
for Time_Step = 1:tau*Fs/length(G_T)
    Pulse=[Pulse Conv_Period];
end
CW=[];
for Time_Step = 1:PRI*Fs/length(G_T)
    CW=[CW Conv_Period];
end
Y_t=conv(G_T,Temp);
Y_t=Y_t(1:length(Temp));
t_tx=0:1/Fs:((length(Y_t)/Fs)-1/Fs);
Time_CW = 0:1/Fs:(PRI-1/Fs);
TX_CW = conv(G_T,CW);
TX_CW = TX_CW(1:length(Time_CW));
TX_Pulsed = conv(G_T,[Pulse zeros(1,length(CW)-length(Pulse))]);
TX_Pulsed = TX_Pulsed(1:length(Time_CW));
TX_Barker = conv(G_T,[Temp zeros(1,length(CW)-length(Pulse))]);
TX_Barker = TX_Barker(1:length(Time_CW));
figure
subplot(3,1,1)
plot(Time_CW,TX_CW)
ylabel('Amplitude'); xlabel('Time [s]'); title('CW TX Signal');
xlim([0 Time_CW(end)/7]); grid on; grid minor;
subplot(3,1,2)
plot(Time_CW,TX_Pulsed)
```

```matlab
ylabel('Amplitude'); xlabel('Time [s]'); title('Pulsed TX Signal');
xlim([0 Time_CW(end)/7]); grid on; grid minor;
subplot(3,1,3)
plot(Time_CW,TX_Barker)
ylabel('Amplitude'); xlabel('Time [s]');
title('Barker Modulated Pulsed TX Signal'); xlim([0 Time_CW(end)/7]);
grid on ; grid minor;
%% Plots
L=2^nextpow2(length(TX_CW)); TX_CW_F=fft(TX_CW)/L;
f=Fs*(0:L/2-1)/length(TX_CW); TX_CW_F=2*TX_CW_F(1:L/2);
TX_CW_F_dB=10*log10(abs(TX_CW_F));

TX_Pulsed_F=fft(TX_Pulsed)/L; TX_Pulsed_F=2*TX_Pulsed_F(1:L/2);
TX_Pulsed_F_dB=10*log10(abs(TX_Pulsed_F));

TX_Barker_F=fft(TX_Barker)/L; TX_Barker_F=2*TX_Barker_F(1:L/2);
TX_Barker_F_dB=10*log10(abs(TX_Barker_F));

figure
subplot(3,1,1)
plot(f/1e6,TX_CW_F_dB)
ylabel('Power [dB]'); xlabel('frequency [MHz]'); title('CW TX Signal');
grid on; grid minor; axis([0 6*Fc/1e6 -30 2]);
subplot(3,1,2)
plot(f/1e6,TX_Pulsed_F_dB)
ylabel('Power [dB]'); xlabel('frequency [MHz]'); title('Pulsed TX Signal');
grid on; grid minor; axis([0 6*Fc/1e6 -40 0]);
subplot(3,1,3)
plot(f/1e6,TX_Barker_F_dB)
ylabel('Power [dB]'); xlabel('frequency [MHz]')
title('Barker Modulated Pulsed TX Signal'); grid on; grid minor
axis([0 6*Fc/1e6 -40 0]);
```

VCO control, PLL and FMCW MATLAB Code

```matlab
clear all; close all; clc
Sweep_BW = 50e6; Sampling_freq = 100e3; % Depending on ADC sampling frequency.
Step_freq = 250e3; Carrier_freq = 5.8e9; % 250 KHz is minimum for the PLL chip.
F=Carrier_freq:Step_freq:Carrier_freq + Sweep_BW;
F_LO = 2.*F; % frequency doubling to RX Harmonic Signal.
V_DAC_Swing = 0:(1/2^12):2.048*(((2^12)-1)/(2^12)); % DAC Full-Scale 2V.
V_Tune_VCO = V_DAC_Swing .* 4; % Required VCO Vtune 4V to 5V.
V_DAC_Res = 1/2^12; % 12-Bit DAC resolution.
TCXO = 30e6; F_PFD = TCXO;
FRAC_N = F./F_PFD;
Prescale = 2; N_Divide = 50;
Paper_Prescale = 2*5*5; % Comparisons with a reference article results.
Ref_VCXO = F./(Prescale*N_Divide*1e6);
Paper_Ref_VCXO = (F./Paper_Prescale)/1e6;
Sweep_time = 10e-3;
```

```matlab
T = 0:Sweep_time/length(F):(Sweep_time)-Sweep_time/length(F);
figure
subplot(2,1,1)
plot(T,Ref_VCXO)
subplot(2,1,2)
plot(T,F)
Fdev = 1e3;
Steps = Sweep_BW/Fdev;
Timer = Sweep_time/Steps;
Fres = F_PFD/2^25;
Res_steps = ceil(Fdev/Fres);
Dev_Off = ceil (log2(Fdev/(Fres*2^15)));
Fdev_res = Fres * 2^(Dev_Off);
Dev = ceil (Fdev/F_PFD *2^(25-Dev_Off));
T_Clk = Timer *F_PFD;
INT = 193; FRAC = 11184811; % Fractional N-divider Settings.
RFout = F_PFD*(INT + (FRAC/2^25));
Target_range = 1:30;
Target_Delay = 2.*Target_range/3e8;
Beat_freq = Sweep_BW.*Target_Delay/Sweep_time;
Range_resolution = 3e8/(2*Sweep_BW);
```

Artwork

B.1   PCB Stack-up Design

PCB stackup

	Copper 17 um Plated to 50 um
	RO4350 508 um
	Copper 17 um
	RO4350 508 um
	Copper 17 um
	RO4350 508 um
	Copper 17 um Plated to 50 um

Via diameter 0.6 mm top to bottom

B.2 Components Placement and Layout
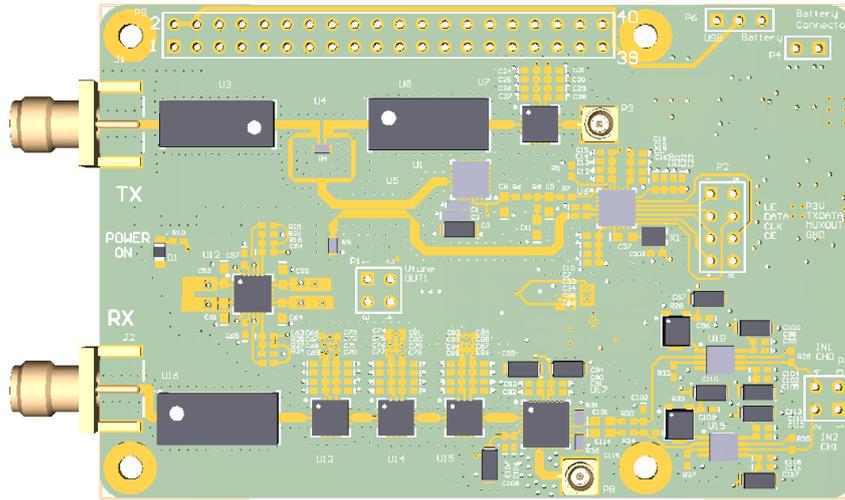
Figure B.1: RF Top Layer Layout.
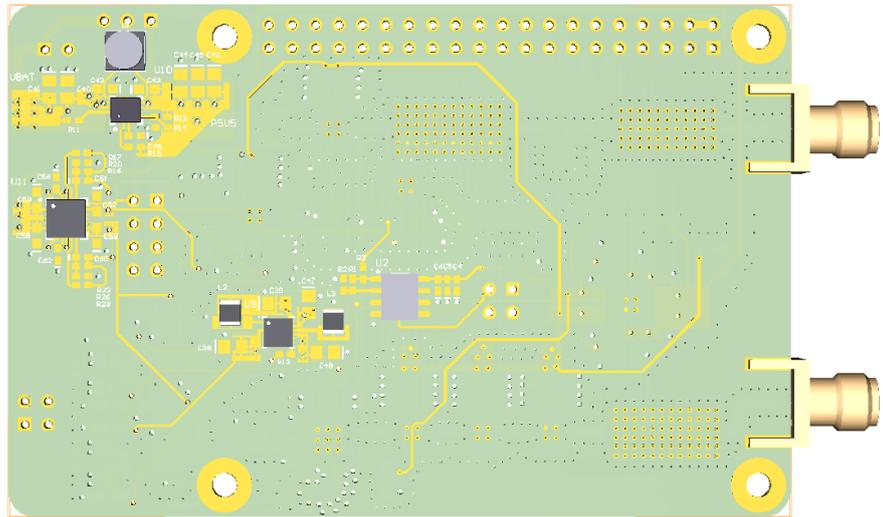
Figure B.2: RF Bottom Layer Layout.

LUND
UNIVERSITY